Computers & Industrial Engineering 206 (2025) 111237

Contents lists available at ScienceDirect

Computers & Industrial Engineering

journal homepage: www.elsevier.com/locate/caie

Optimising timing points for effective automatic train operation

Ziyulong Wang [a],*, Egidio Quaglietta [a], Maarten G.P. Bartholomeus [b], Alex Cunillera [a], Rob M.P. Goverde [a]

[a] Department of Transport and Planning, Delft University of Technology, P.O. Box 5048, 2600 GA Delft, The Netherlands
[b] Department of ERTMS Central Systems, ProRail, P.O. Box 2038, 3511 EP Utrecht, The Netherlands

ARTICLE INFO

Keywords:
Timing points
Automatic train operation
Train Path Envelope
Train driving strategies

ABSTRACT

Automatic Train Operation (ATO) aims to partially or fully automate train driving, enhancing railway capacity, punctuality, and energy efficiency. However, a key challenge arises from the mismatch between discrete event-time decisions at the Traffic Management System (TMS) level, assuming fixed running times, and the continuous speed–distance trajectory optimisation at the ATO level, leading to possible misalignments between planned and executed train movements. To bridge this gap, this paper introduces a novel optimisation-based method that dynamically computes Train Path Envelopes (TPEs) based on multiple driving strategies, defined as time targets or windows over a sequence of timing points, which ATO-equipped trains must comply with to align their movements with traffic management constraints. The method follows a two-stage approach: First, a linear programming model determines conflict-free blocking time ranges across the multiple driving strategies. Second, a structured optimisation process establishes operationally feasible TPEs by determining departure tolerances and configuring intermediate timing points. By integrating a critical-block strategy, the optimised TPEs provide the flexibility needed for ATO while accommodating variations in train driving strategies. The method is validated through experiments and a real-life case study in The Netherlands, demonstrating that optimised timing points at critical track locations improve energy efficiency, enhance punctuality, increase capacity, and provide an approach to align traffic management with ATO.

1. Introduction

The increasing demand for railway transport has led to a nearly saturated condition in many heavily used railway networks worldwide. Besides deploying advanced signalling systems, the railway sector proposes Automatic Train Operation (ATO) to address this issue (EU-RAIL, 2022). ATO automates train driving partially or fully to reduce the impact of human factors on railway operations, enhancing punctuality, energy efficiency, and capacity (Yin et al., 2017). In particular, ATO can reduce the variations in train running times or dwell times. These processes are now heavily affected by human behaviour, e.g., the driving style of a human train driver or the passenger interactions at platforms when boarding/alighting the trains, respectively (Jansson et al., 2023). With ATO, train driving and dwell times become more predictable.

Hitherto, most literature has focused on developing a railway Traffic Management System (TMS) that generates a real-time traffic plan—defining train routes, reference locations and times, and possible rescheduling strategies—for train operation (Corman & Meng, 2015), or explores the integration of TMS and ATO (Rao et al., 2016). Recent technological developments partition ATO into onboard and trackside components with a standardised communication interface to exchange information dynamically to support or automate train driving (Wang, Z. et al., 2022). To align ATO with timetable-based traffic management, the real-time traffic plan from the TMS must be translated into a sequence of Timing Points (TPs) at successive track locations, with time targets or windows for each connected train to facilitate onboard trajectory generation and tracking. These TPs and their associated time windows or targets are assembled in a Train Path Envelope (TPE) as proposed in the literature (Quaglietta et al., 2016; Wang, P. & Goverde, 2016, 2017). The onboard ATO algorithm uses this TPE as constraints for train trajectory generation. State-of-the-art research mainly focused on developing approaches for punctual and energy-efficient ATO onboard algorithms (Huang et al., 2018; Yin et al., 2017), whereas a literature gap remains in the definition and modelling of the TPE and its associated TP location and time constraints. In particular, no approach has been developed to optimise the TPs in a TPE for successive trains. Nevertheless, the TP configurations are critical to instruct the onboard

* Corresponding author.
E-mail addresses: z.wang-19@tudelft.nl (Z. Wang), e.quaglietta@tudelft.nl (E. Quaglietta), maarten.bartholomeus@prorail.nl (M.G.P. Bartholomeus), a.cunilleraperez@tudelft.nl (A. Cunillera), r.m.p.goverde@tudelft.nl (R.M.P. Goverde).

https://doi.org/10.1016/j.cie.2025.111237
Received 15 December 2023; Received in revised form 27 March 2025; Accepted 13 May 2025
Available online 28 May 2025

algorithms effectively to follow the real-time traffic plan without track occupation conflicts.

Typically, conflict-free timetabling models assume a deterministic time–distance train path (Caimi et al., 2011; Goverde et al., 2016; Wang P. et al., 2022; Zhang et al., 2019), as do timetable rescheduling approaches applied in a TMS (Corman et al., 2010; Li et al., 2023; Pellegrini et al., 2014; Quaglietta et al., 2016). In contrast, a train may operate with various train driving strategies that all satisfy scheduled departure and arrival times, such as following a scheduled cruising speed or applying energy-efficient train control (Scheepmaker et al., 2020). These variations lead to a range of train passing times, potentially causing conflicts between successive trains adopting different driving strategies. To this end, the main objective of TPE computation is to provide the ATO onboard with an optimal TP configuration, i.e., a set of TPs with corresponding time constraints, that respects scheduled station arrivals while allowing sufficient flexibility to accommodate uncertainties in train driving strategies and prevent conflicts between successive trains.

Building on this, we consider the following research question: How can TPEs be computed to ensure conflict-free operations of ATO-equipped trains? This question is further broken down into three sub-questions: How can we identify possible misalignment between the TMS real-time traffic plan and ATO speed profile generation to ensure feasibility and conflict-free operations? How can the locations and time windows of TPs in a TPE be determined effectively while accounting for variability in ATO driving strategies? How does the proposed approach impact railway operations in a real-world case study?

We address these research questions by proposing an innovative TPE computation method that dynamically determines optimised TPs and associated time windows to enable punctual, conflict-free and energy-efficient train operation while allowing flexibility in the adopted ATO onboard driving strategies. Specifically, for each train, we compute a range of blocking times across successive blocks, corresponding to multiple train driving strategies that may be adopted during operation. Critical TPs and time bounds are derived to avoid blocking time conflicts between trains, achieving robustness against uncertainties in train driving strategies and maintaining compliance with the real-time traffic plan. We test and verify the developed model in various experiments and demonstrate its potential in a case study on one of the busiest Dutch railway corridors with heterogeneous traffic. Results from a real-life case study show that the critical-block TP configuration, which forms the TPE, outperforms alternative approaches, such as using only TPs at scheduled stops or successively adding TPs based on the first conflicting block in an iterative manner.

The contributions of our paper are summarised as follows:

- We introduce the concept of a train path envelope by considering multiple train driving strategies to manage uncertainties in train trajectory modelling and enhance alignment between traffic management and train operation.
- We develop a two-stage optimisation-based method to compute train path envelopes, incorporating a critical-block timing point determination approach to guide ATO-driven trains in generating conflict-free, energy-efficient and punctual train trajectories.
- The proposed method is validated on one of the busiest Dutch heterogeneous railway corridors, demonstrating its feasibility and practical applicability.

The proposed method can also be extended to other domains where automated processes must adhere to time targets or windows, ensuring time- and energy-efficient execution of a predefined timetable, such as in aviation, supply chain management, and road transport. The remainder of this paper is organised as follows: Section 2 offers an overview of the related works and entails the research gaps, followed by Section 3 where the methodological framework is presented. Then, Section 4 describes the case study and discusses the results. Section 5 provides managerial insights and examines the applicability and limitations of the proposed approach. Finally, Section 6 summarises the key findings and outlines future research directions.

2. Related works

Rail traffic optimisation can be generally classified into two groups (Rao et al., 2016): On the one hand, the TMS monitors and predicts the status of traffic and infrastructure, detects and resolves train path conflicts, and ultimately computes the real-time traffic plan for train operations. On the other hand, ATO aims to generate and track an optimal train trajectory to respect the real-time traffic plan and provide the resulting real-time traction and brake commands to control the train speed effectively.

Yet, traffic management and train operation have been considered separately for quite a long time in mainline railways (Rao et al., 2016). The concept of a TPE was proposed in the literature to bridge these two based on the input of a (re)scheduled traffic plan from the TMS. A TPE defines a sequence of time targets or windows at TPs, ensuring conflict-free train operation while enabling train trajectory optimisation and maintaining schedule punctuality (Albrecht, T. et al., 2013; Quaglietta et al., 2016). So far, it has been successfully implemented in train trajectory optimisation (Wang, P. & Goverde, 2016; Wang, P. et al., 2020). Table 1 provides an overview of existing studies on the interaction between traffic management and train operation at the operational planning stage, with a particular focus on the role of TPE in bridging these two domains. The TPE is part of a Journey Profile that is sent from the trackside to the train onboard systems within ATO and Connected Driver Advisory Systems (C-DAS) architectures (Wang, Z. et al., 2022). The ATO onboard then generates a train trajectory satisfying the constraints in the TPE to automatically operate the train.

In essence, a TPE defines time bounds at TPs to ensure sufficient separation between trains (Albrecht, A.R. et al., 2015; Haahr et al., 2017). We refer interested readers to the review paper by Scheepmaker et al. (2017) for the state-of-the-art of energy-efficient train trajectory optimisation. Recent works have further explored trajectory optimisation by using Quadratically Constrained Linear Programming-based (Ying et al., 2023) and analytical solutions (Howlett et al., 2023) to explicitly handle time constraints at TPs. Notwithstanding, few studies focus on optimising the TPE per se. Specifically, the time targets or windows defined according to the scheduled departures and arrivals at stops may not be sufficient to guarantee conflict-free train trajectories during operations when the train trajectories between two stations are modelled deterministically. Hence, Wang, P. and Goverde (2017) and Wang, P. and Goverde (2019) devised the concept of a Timetable Constraint Set to fine-tune the values of time and speed windows based on operability, feasibility, and energy efficiency.

An optimal interaction between traffic management and train operation is required to control the train speed to avoid train path conflicts and minimise the impact of disturbances. Rao et al. (2016) provided an integrated approach that collectively considered the TMS and ATO to generate a set of conflict-free train trajectories with a focus on the speed control of each train. Luan et al. (2018a) modelled the train speeds as decision variables to minimise the total delay and employed three optimisation methods. Among these three approaches, a two-level pre-processing speed profile generation and selection method performed best and was extended further to energy reduction (Luan et al., 2018b). Along the same research line, Long et al. (2023) proposed a mixed-integer linear programming model to simultaneously determine train orders, routes, departure and arrival times, as well as speed profiles, allowing for a precise representation of the effect and dynamics of temporary speed restrictions on high-speed railways. Continuing the development of integrating traffic management and train operation in high-speed rail, Dong et al. (2022) proposed an online rescheduling framework for real-time disruption management, integrating train rescheduling and speed trajectory optimisation to enhance operational recovery. Dong et al. (2024) introduced a reinforcement learning-based approach that integrates train trajectory optimisation with timetable rescheduling to minimise delays and energy consumption, using rescheduled train running times as the bridge between

Table 1
Overview of the relevant studies on the connections between traffic management and train operation at the operational planning stage.

Author (s)	Main focus	Railway type	Objectives	Connections between traffic management and train operation
Albrecht, T. et al. (2013)	Train trajectory optimisation	Mainline	Delay minimisation; Energy efficiency	Target point; Target window
Albrecht, A.R. et al. (2015)	Train trajectory optimisation	Mainline	Energy efficiency	Passage point
Quaglietta et al. (2016)	Real-time traffic management	Mainline	Conflict detection and resolution; Energy efficiency	Train Path Envelope
Rao et al. (2016)	Integrated traffic management and train operation	Mainline	Conflict detection and resolution; Energy efficiency	Main-target point; Sub-target point
Wang, P. and Goverde (2016)	Train trajectory optimisation	Mainline	Delay minimisation; Energy efficiency	Train Path Envelope
Haahr et al. (2017)	Train trajectory optimisation	Mainline	Energy efficiency	Passage point
Wang, P. and Goverde (2017)	Train trajectory optimisation	Mainline	Delay minimisation; Energy efficiency	Timetable constraint set
Luan et al. (2018a)	Integrated traffic management and train operation	Mainline	Delay minimisation	Train speed
Luan et al. (2018b)	Integrated traffic management and train operation	Mainline	Delay minimisation; Energy efficiency	Train speed
Hou et al. (2019)	Integrated traffic management and train operation	Metro	Delay minimisation; Energy efficiency; Demand satisfaction	Speed profile selection
Mo et al. (2019)	Integrated traffic management and train operation	Metro	Demand satisfaction; Energy efficiency	Speed profile selection
Wang, P. and Goverde (2019)	Train trajectory optimisation; Energy-efficient timetabling	Mainline	Conflict detection and resolution;Energy efficiency	Timetable constraint set
Wang, P. et al. (2020)	Train trajectory optimisation	Mainline	Parametric uncertainty minimisation; Time and energy cost	Train Path Envelope
Li et al. (2021)	Integrated traffic management and train operation	Metro	Headway regularity; Energy efficiency	Train headway time; Speed profile selection
Dong et al. (2022)	Integrated traffic management and train operation	High-speed	Delay minimisation; Energy efficiency	Train running time; Train trajectory
Wang, Y. et al. (2022)	Integrated traffic management and train operation	High-speed	Delay minimisation; Energy efficiency	Train running time; Train dwell time
Howlett et al. (2023)	Train trajectory optimisation	Mainline	Safe separation; Energy efficiency	Target time
Liu et al. (2023)	Integrated traffic management and train operation	Metro	Passenger travel time; Energy efficiency	Train timetable; Speed profile selection
Long et al. (2023)	Integrated traffic management and train operation	High-speed	Delay minimisation	Train speed
Ying et al. (2023)	Train trajectory optimisation	High-speed	Energy efficiency	Target window
Dong et al. (2024)	Integrated traffic management and train operation	High-speed	Delay minimisation; Energy efficiency	Train running time
This paper	Timing Point and Train Path Envelope optimisation	Mainline	Timetable-trajectory alignment; Timetable robustness; Driving flexibility; Delay minimisation; Energy efficiency	Train Path Envelope

the two processes. Additionally, Wang, Y. et al. (2022) developed a hierarchical model predictive control method to jointly manage delays and train speed control, where train running and dwell times act as the key linking factors.

Besides, metro systems have widely implemented ATO and mostly adopted this integrated concept (Yin et al., 2017). Usually, the goal is to minimise energy consumption by collectively considering the timetable and the speed profiles. Hou et al. (2019) and Mo et al. (2019) aimed to select the most suitable speed profile out of a pre-generated set for optimising the energy-efficient train operation and scheduling. Furthermore, Li et al. (2021) integrated the dwell time regulation in the timetable with the speed profile selection to enhance the real-time metro system performance. Liu et al. (2023) developed a bi-level model predictive control approach that simultaneously adjusts train schedules and speed profiles based on time-dependent passenger origin–destination demand.

However, ATO development in mainline railways necessitates a distinction between traffic management and train operation due to the vertical separation of railways between infrastructure manager and railway undertaking in European Union member states (Nash et al., 2014). Moreover, the TMS and ATO represent different dynamics and scopes. On the one hand, the TMS reschedules a timetable in case of disturbances and disruptions, focusing on optimal track capacity allocation and travel times on the network level. On the other hand, ATO regulates the trains by computing feasible and energy-efficient speed trajectories over the assigned routes within the margins contained in the real-time traffic plan. Such a discrepancy introduces uncertainty in train running and dwell times, making train timetable (re)scheduling increasingly complex to solve while strongly affecting both the quality and robustness of the timetable (Zhan et al., 2024). Consequently, directly controlling the train from a TMS cannot be realised, while determining an optimised set of TPs with temporal constraints along the train route is of utmost necessity to bridge TMS and ATO in the system architecture aforementioned.

Overall, the existing studies are mostly limited to adopting the TPE and similar concepts as constraints for train trajectory optimisation. No existing study provides a method for optimising TP locations with their associated time targets or windows in a TPE to ensure conflict-free train trajectory generation. Nonetheless, this optimisation is crucial for ATO implementation to fully realise its benefits, including enhanced capacity, punctuality, and energy efficiency. The first attempt to compute the TPEs was based on splitting the buffer time between trains at selected locations into two halves and then allocating a half to the time window of each of two successive trains (Wang, P. & Goverde, 2016). Wang, P. and Goverde (2017, 2019) proposed the concept of a Timetable Constraint Set to fine-tune the time and speed windows, although they considered the TPs only at stations while focusing on multi-train trajectory optimisation.

The challenges of determining TPs in a TPE mainly arise from three aspects: First, multiple train driving strategies could be applied for the same running time between two stops, which leads to uncertainty of train trajectory modelling in the TMS. Second, the computation of conflict-free TPEs for successive trains is still an open problem. Even with a (re)scheduled timetable, operational conflicts may still arise due to variations in train driving behaviour. Therefore, merely following the target time at stops based on an assumed deterministic train time–distance path cannot ensure conflict-free train operations. Third, defining TPs and their associated time windows requires balancing flexibility in train driving strategies with adherence to the real-time traffic plan. A rigid set of TPs may not accommodate variations in train operations, potentially leading to track occupation conflicts, whereas an excessive number of TPs could overly constrain flexibility, reducing ATO adaptability and energy efficiency. As a result, this paper proposes a new method to guide the trains within conflict-free TPEs by identifying an optimal sequence of TPs and associated time windows for each train. Our approach thus contributes to the identified and required future works to interface the TMS, ATO trackside, ATO onboard, and the signalling systems in mainline railways (Goverde et al., 2023) and serves as a cornerstone within the Europe's Rail FP1-MOTIONAL project, which includes efforts to align and enhance the interaction between TMS and ATO (EU-RAIL, 2024).

3. Methodology

This section begins with a problem description and key assumptions that form the foundation of the proposed modelling framework (Section 3.1). Next, Train Path Slot and TPs are introduced based on blocking time theory and multiple train driving strategies in Section 3.2, followed by the complete modelling framework with five modules in Section 3.3 to determine an optimised set of TPs. Lastly, the evaluation criteria for quantifying the results are in Section 3.4.

3.1. Problem description and assumptions

Effective ATO deployment requires seamless alignment between the network-wide real-time traffic plan and real-time train trajectory generation and tracking. The TMS (re)schedules train timetables (times, orders, routes) at the traffic level in response to disturbances and disruptions, whereas the ATO onboard functions at the individual train level, generating and tracking train trajectories (speed over distance) to ensure compliance with operational constraints. However, existing approaches lack a mechanism to dynamically synchronise ATO-driven trajectory generation with timetable-based traffic management, leading to possible misalignments between planned and actual train time–distance trajectories.

This misalignment is particularly pronounced in mainline railways, where the TMS does not directly control train speed, and train trajectory generation depends on dynamic ATO driving strategies. Timetable (re)scheduling models typically determine discrete arrival and departure times at selected timetable points, assuming deterministic (minimum) running times to ensure theoretical conflict-freeness. However, trains may adopt different driving strategies—such as maintaining a target timetable speed or employing energy-efficient control with cruising and coasting regimes—resulting in different continuous speed–distance trajectories between the discrete scheduled timing points, while still adhering to the same computed timetable. This variability results in different time–distance trajectories between stops, introducing operational uncertainties that can cause train path conflicts, particularly for successive trains sharing track resources.

This study proposes a TPE computation method as an interface between the TMS real-time traffic plan and ATO onboard speed control. This method dynamically determines possible locations where trains may have track occupation conflicts due to incompatible driving strategies and derives extra timing points with associated time constraints to prevent these conflicts. These extra timing points are subsequently collected together with the scheduled event times at the timetable points as an ordered list of time constraints in a TPE for each train. The TPE is then sent to the ATO onboard to guide ATO-driven trains toward conflict-free, punctual, and energy-efficient operations while preserving flexibility in train trajectory generation.

The following key assumptions are used in our approach: (1) The TMS provides a conflict-free real-time traffic plan that specifies scheduled departure and arrival times at designated stops, train routing, and the predefined train precedence order; (2) Trains can adopt different driving strategies (e.g., minimum-time, scheduled-speed, or energy-efficient control), leading to a range of possible passing times between stops; (3) This study assumes a fixed-block signalling system with continuous braking curve supervision (e.g., European Train Control System (ETCS) Level 2) as an example. However, the methodology applies to any signalling system, such as conventional multi-aspect and moving-block signalling systems, with the blocking time computations adapted accordingly; (4) Regenerative braking is not explicitly modelled, but the methodology can be extended to incorporate energy-efficient train control with regenerative braking (Scheepmaker & Goverde, 2020), as any other valid driving strategy, without loss of generality; (5) We assume that data communication follows standard railway telecommunication specifications, such as GSM-R used in ETCS Level 2.

3.2. Train Path Slot and timing points

The railway infrastructure can be regarded as a series of block sections that are allocated exclusively to one train at a time, during which it is blocked for other trains (Pachl, 2014). The successive blocking times of each train over a railway corridor in a time–distance graph are the so-called blocking time stairway in which the blocking times can be seen as boxes of time slots over the blocks (Goverde et al., 2013). If on a block section, the blocking times of two successive trains overlap, then a conflict would occur and thus will result in unnecessary braking and possibly stopping until the block is released. Otherwise, the white space between two consecutive trains for each block (i.e., the buffer time) can be leveraged to optimise the train trajectory as long as there is no overlap.

Nevertheless, the blocking time stairway could vary for the same departure and arrival time as the running time in a specific intermediate block section differs among train driving strategies. In particular, the conflict detection and resolution algorithms in a TMS typically rely on a deterministic train path based on a single train trajectory. The inconsistency of the train driving strategies utilised by the traffic management and the train operation leads to different intermediate passing times, which might result in train path conflicts. As a result, we define the concept of a Train Path Slot as an integrated blocking time stairway pattern based on multiple driving strategies, specifying the successive passing windows of each train over a railway corridor. In this paper, we propose three driving strategies: shifted Minimum-Time Train Control (MTTC), Reduced Maximum Speed (RMS, a reduced cruising speed without coasting) and Energy-Efficient Train Control (EETC, combining cruising and coasting), see Section 3.3.1. The shifted MTTC considers a late departure tolerance (i.e., an allowed late departure window) equal to the available running time supplement until the next arrival time. It drives the train as fast as possible and respects the imperative target scheduled arrival time at the next stop. The late departure

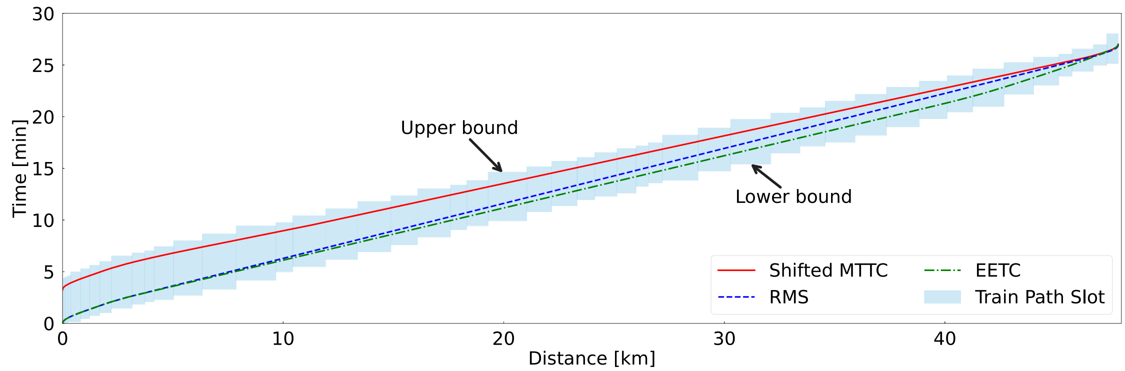

Fig. 1. Example of a Train Path Slot.

tolerance represents a further robustness of the scheduled train paths. This strategy provides some flexibility on the departure time due to, for instance, extended boarding. The derived trajectories based on these driving strategies determine the initial lower and upper bounds of the Train Path Slot, i.e., without yet considering the adjacent trains as detailed in Section 3.3.2. We present an example of an initial Train Path Slot in Fig. 1. These preliminary Train Path Slots can reveal potential train path conflicts inherently contained in the real-time traffic plan as they take the time–distance paths from different speed profiles into account.

Train Path Slots for successive train pairs may overlap and must be resolved to ensure conflict-free operations, forming the basis for an optimised set of TPs. If no overlap occurs, the scheduled arrival time and a departure tolerance up to the running time supplement define the optimised TPs for a train run. Conflict-free Train Path Slots are achieved by considering all adjacent trains and applying Train Path Slot overlap detection and resolution in Sections 3.3.3 and 3.3.4. To resolve conflicts, we formulate a Linear Programming (LP) model that identifies successive conflict-free blocking time windows. This LP model serves as the first stage of a two-step process, where a subsequent computation stage ensures train trajectory feasibility by refining departure tolerances and introducing intermediate TPs. The LP model prioritises adjusting the departure tolerance for the preceding train in a train pair and then imposes constraints on the nominal driving of a following train. Here, nominal driving refers to train operation that adheres to the scheduled departure and arrival times from the plan. The outcome of the LP model is a set of conflict-free Train Path Slots without considering the train dynamics, i.e., the train has to provide a corresponding train trajectory to respect these slots and make them feasible. Therefore, TPs are configured at the entry location of the blocks to ensure that realisable train time–distance profiles are kept within the identified conflict-free Train Path Slots. We propose a critical-block TP configuration that introduces a TP to the block having the largest overlapping blocking time. It is compared with other alternatives of only using TPs at scheduled stops or successively adding TPs based on the first conflicting block in an iterative approach in the case study.

The train driving strategies that meet the optimised lower and upper bounds of a restricted Train Path Slot from the LP model are called a TP response strategy and a departure tolerance response strategy, respectively. These two driving strategies are established to respect the optimisation results and provide feasible event times at TPs as constraints for any onboard train trajectory optimisation approaches, i.e., departure, arrival and passing times. Specifically, the TP response strategy is defined as a combination of RMS and EETC driving strategies with possibly multiple response cruising speeds to avoid Train Path Slot overlaps. The departure tolerance response strategy relies on the RMS driving strategy. It starts at the adjusted departure tolerance such that the remaining running time supplement is the scheduled running time supplement minus the departure tolerance. This adjusted departure tolerance will always be smaller than the given running time supplement because the initial departure tolerance was defined as the running time supplement for the shifted MTTC to arrive at the scheduled arrival time at the next stop. The discrete TPs with either time targets or windows are eventually assembled into the TPE in Section 3.3.5. The reduction of a restricted Train Path Slot with an optimised set of TPs in a TPE as the output of our modelling framework is visualised on the right-hand side of Fig. 5.

3.3. Modelling framework

The proposed modelling framework uses four types of data, i.e., timetable, route, signalling and rolling stock characteristics. The framework is provided as a flow diagram in Fig. 2 and consists of five modules, with Train Path Slot overlap resolution following a two-step approach: (1) an LP model that determines conflict-free Train Path Slots, and (2) a response train trajectory generation stage that ensures feasible operations by adjusting departure tolerances and introducing intermediate TPs, ultimately forming the TPE. The five modules are: (1) Train trajectory computations for three relevant train driving strategies, (2) Train Path Slot computation by using blocking time theory, (3) Train Path Slot overlap detection, (4) Train Path Slot overlap resolution through utilising TPs, (5) TPE construction with an optimised set of TPs. Each step feeds into the next, forming the TPE computation process. The following subsections manifest each of the modules, sequentially. We also provide the notation used in this paper in Table 2.

3.3.1. Train trajectory computation

Train trajectories are computed in two stages: first, using different driving strategies to establish initial Train Path Slots, and later, re-computed as response driving strategies to satisfy the LP model's conflict-free Train Path Slot constraints. In this second stage, response driving strategies determine the actual departure tolerances and passing times at intermediate TPs, which together form the TPE. The train trajectory modelling is train-specific and incorporates train-specific parameters, including traction characteristics, braking rates, and mass.

Our train trajectory computation considers three train driving strategies, the shifted MTTC, the RMS and the EETC. The shifted MTTC train driving strategy is based on the MTTC train driving strategy that operates the train as fast as possible with a departure tolerance. This departure tolerance corresponds to departing late up to the running time supplement. The original MTTC train driving strategy is used in the timetable design to compute the minimum running time, and based on that, determine the additional running time supplement. By applying Pontryagin's Maximum Principle and the Karush–Kuhn–Tucker conditions, we are able to derive the optimal control structure of the MTTC problem as detailed in Albrecht, A.R. et al. (2016a) and Goverde et al. (2021) and then produce the MTTC speed profile. The resulting driving strategy consists of three driving regimes: maximum acceleration of

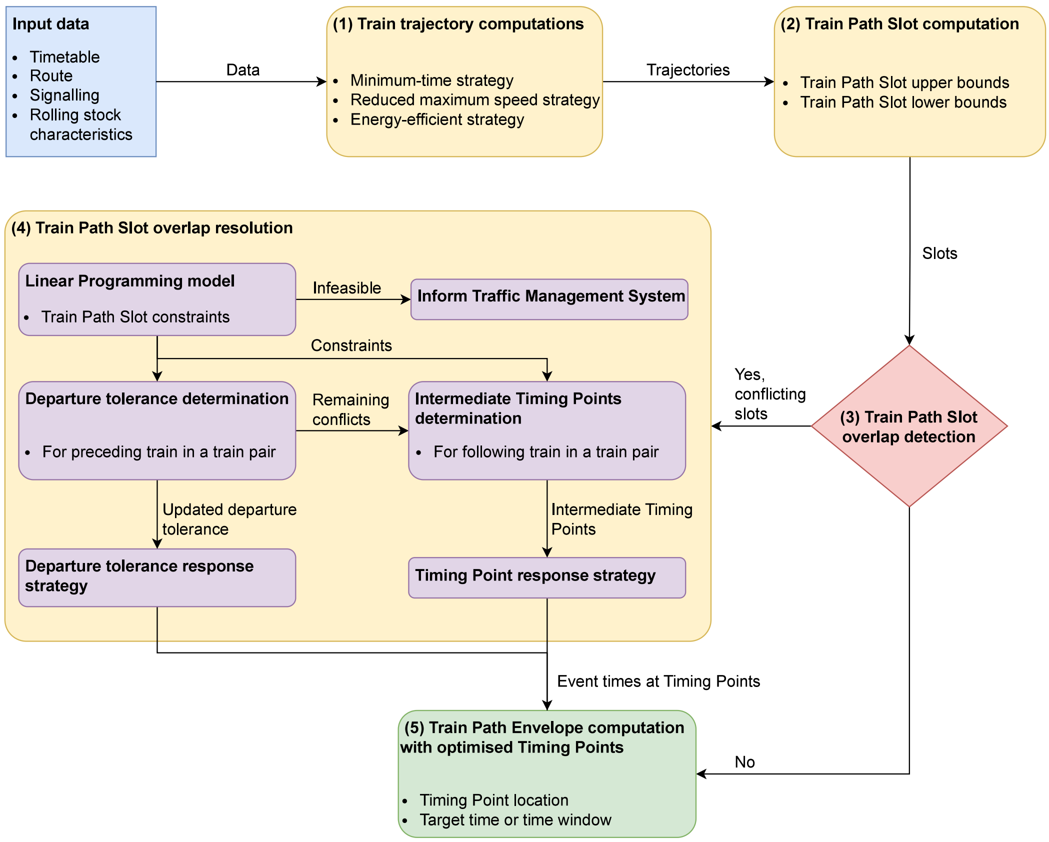

Fig. 2. Methodological framework of optimised Timing Points for ATO.

the train until reaching the speed limit, cruising at the speed limit (if reached), and service braking. If there are varying speed limits between two stops, the train has to apply service braking or maximum acceleration to transition between different cruising speeds at these speed limits.

The other two strategies, RMS and EETC, use the full scheduled running time between scheduled departure and arrival times. The EETC driving strategy aims to minimise the total energy consumption between two stops. Its optimal control structure is well-established in Albrecht, A.R. et al. (2016b) and Goverde et al. (2021). Again, we can obtain the optimal control structure of the EETC problem by using Pontryagin's Maximum Principle and the Karush–Kuhn–Tucker conditions and then generate the EETC speed profile. The resulting driving strategy comprises four driving regimes: maximum acceleration of the train until reaching the optimal cruising speed, cruising at the optimal cruising speed, coasting without using the engine or brakes of the train, and service braking. The RMS driving strategy is based on a scheduled cruising speed without coasting, which adds a restrictive constraint on top of the EETC control structure to avoid the coasting regime (Scheepmaker et al., 2020). Thus, its resulting driving strategy only has three driving regimes: maximum acceleration of the train until reaching the optimal cruising speed (when no coasting is used), cruising at the optimal cruising speed, and service braking. The RMS essentially determines a timetable speed that trains can maintain to arrive on time, which is a typical running time calculation assumption in timetable planning.

We visualise an example of a speed–distance diagram (i.e., speed profile) of these three driving strategies in Fig. 3. All three driving strategies comprise regimes of maximum acceleration and service braking. The MTTC (in solid red) cruises at the speed limit (in solid black), whereas the RMS (in dashed blue) cruises at a required cruising speed to arrive on time. With the same amount of running time supplement, the EETC (in dash-dotted green) has a higher cruising speed than the RMS due to the following coasting regime. Moreover, the grey area in the figure indicates the track gradient profile.

3.3.2. Initial Train Path Slot computation

This subsection determines the lower and upper bounds of a Train Path Slot based on the computed train trajectories, which represent the start and end times of the blocking time stairway diagrams. Specifically, we take the train trajectories with one of the three train driving strategies as input and build the corresponding blocking time stairways. Then, we select the most critical boundaries of the blocking time stairways as the bounds of the Train Path Slot to obtain this integrated blocking time stairway pattern. In general, the shifted MTTC and the EETC driving strategies determine the upper and lower bounds of a Train Path Slot, respectively. Nevertheless, there could be exceptions.

We compute the Train Path Slot lower bound by building the blocking time diagrams based on the shifted MTTC, RMS and EETC driving strategies and selecting the earliest time at any block between two stops. For shifted MTTC driving, we assume that the train exhausts all the running time supplement r_p before departing between two stops while the other two depart as scheduled. All three driving strategies follow the scheduled arrival times. Let P be the set of trains. In ETCS Level 2, the approach distance of train $p \in P$ before block b is the absolute braking distance, depending on the train, route and speed. We use the resulting braking time plus a safety margin to indicate the approach time $t^{\text{approach}}_{p,b}$. Hence, the lower bound (denoted by the underscore) of the Train Path Slot $\underline{t}^{\text{TPS}}_{p,b}$ is the earliest reserved time of train p at the entrance point of a block b among all three driving strategies:

$$\underline{t}^{\text{TPS},\gamma}_{p,b} = \sum_{b' \in B_{p,b}} t^{\text{run},\gamma}_{p,b'} - t^{\text{approach},\gamma}_{p,b} - t^{\text{reaction}}_{p,b} - t^{\text{setup}}_{p,b}, \qquad \gamma \in \{\text{RMS, EETC}\}, \tag{1}$$

Table 2
Notation used in this paper.

Symbols	Definitions
Sets (predefined)	
P, p	P is a set of trains, and p is a train within P
P_2, (p_i, p_j)	$P_2 = \{(p_i, p_j) \mid p_i, p_j \in P, p_i \prec p_j\}$ is a set of successive train pairs with p_i preceding p_j before a possible scheduled Overtaking, and (p_i, p_j) is a train pair within P_2
B_p, b	B_p is a set of blocks along the route of train p with an ordering $B_p = \{b_1, \dots, b_n\}$, and b is a block within B_p
B_p^{parallel}, b	B_p^{parallel} is a set of successive blocks of train p on a track of multiple-track line(s), and b is a block within B_p^{parallel}
$B_{p,b}$, b'	$B_{p,b} \subset B_p$ is a set of blocks that train p has traversed before block b, and b' is a block within $B_{p,b}$
S'_p, s_b	S'_p is a set of all possible Timing Points at the entry location of a block in the running direction of train p, and $s_b \in S'_p$
Γ, γ	Γ is a set of train driving strategies, and γ is a driving strategy within Γ
TPS_p	TPS_p is the Train Path Slot of train p, $\text{TPS}_p = \left\{ \left(b, \underline{t}_{p,b}^{\text{TPS}}, \bar{t}_{p,b}^{\text{TPS}} \right), b \in B_p \right\}$
Fixed parameters	
r_p	Running time supplement of train p between two stops
$t_{p,b}^{\text{setup}}$	Setup time of the route for train p in block b
$t_{p,b}^{\text{reaction}}$	Sight and reaction time of train p in block b
$t_{p,b}^{\text{release}}$	Release time of train p to free up block b
t_p^{buffer}	Buffer time in the timetable to prevent delay propagation as part of the Train Path Slot upper bound of train p
$\alpha_{p_i,p_j,b}$	Binary parameter to specify whether train p_i precedes p_j in block b. If yes, $\alpha_{p_i,p_j,b} = 1$; otherwise, $\alpha_{p_i,p_j,b} = 0$
Variables	
$c_{p_i,p_j,b}$	Train Path Slot overlap between trains p_i and p_j in block b
$c_{p_i,p_j}^{\max}$	Largest Train Path Slot overlap between trains p_i and p_j in a chosen railway corridor
$\underline{t}_{p,b}^{\text{TPS},\gamma}$	Lower bound of the Train Path Slot in block b for train p based on a driving strategy γ
$\bar{t}_{p,b}^{\text{TPS},\gamma}$	Upper bound of the Train Path Slot in block b for train p based on a driving strategy γ
$\underline{t}_{p,b}^{\text{TPS}}$	Initial lower bound (i.e., the reserved time) of the Train Path Slot in block b for train p
$\bar{t}_{p,b}^{\text{TPS}}$	Initial upper bound (i.e., the end time) of the Train Path Slot in block b for train p
$t_{p,b}^{\text{approach},\gamma}$	Approach time of train p for block b based on a driving strategy γ
$t_{p,b}^{\text{run},\gamma}$	Runing time of train p in block b based on a driving strategy γ
$t_{p,b}^{\text{clear},\gamma}$	Clearing time of train p for block b based on a driving strategy γ
Decision variables of the LP model	
$x_{p,b}$	Time of the optimised Train Path Slot lower bound of train p in block b
$y_{p,b}$	Time of the optimised Train Path Slot upper bound of train p in block b
Sequentially optimised sets and variables	
S_p, s	S_p is a set of Timing Points of train p, and s is a Timing Point within S_p
TPE_p	TPE_p is the Train Path Envelope of train p, $\text{TPE}_p = \left\{ \left(s, t_{p,s}^{\min}, t_{p,s}^{\max} \right), s \in S_p \right\}$
$\text{TPS}_p^{\text{cons}}$	$\text{TPS}_p^{\text{cons}}$ is the Train Path Slot constraint of train p, $\text{TPS}_p^{\text{cons}} = \left\{ \left(b, x_{p,b}, y_{p,b} \right), b \in B_p \right\}$
$t_{p,s}^{\min}$	Earliest time for train p to arrive at Timing Point s
$t_{p,s}^{\max}$	Latest time for train p to arrive at Timing Point s
τ_p^{D}	Departure tolerance of train p
$\hat{\tau}_p^{\text{D}}$	Restricted departure tolerance of train p

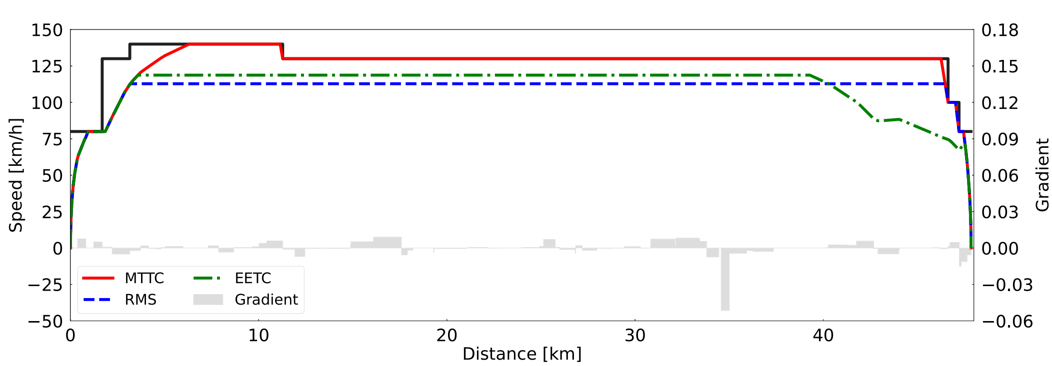

Fig. 3. Example of the Minimum-Time Train Control (MTTC), Reduced Maximum Speed (RMS) and Energy-Efficient Train Control (EETC) driving strategies.

$$\underline{t}_{p,b}^{\text{TPS},\gamma} = r_p + \sum_{b' \in B_{p,b}} t_{p,b'}^{\text{run},\gamma} - t_{p,b}^{\text{approach},\gamma} - t_{p,b}^{\text{reaction}} - t_{p,b}^{\text{setup}}, \qquad \gamma = \text{MTTC}, \tag{2}$$

$$\underline{t}_{p,b}^{\text{TPS}} = \min_{\gamma \in \Gamma} \left(\underline{t}_{p,b}^{\text{TPS},\gamma} \right), \tag{3}$$

where the set $\Gamma = \{\text{MTTC, RMS, EETC}\}$ represents the set of the three driving strategies and the set $B_{p,b} \subset B_p$ represents the set of blocks before b that train p has traversed. $t_{p,b'}^{\text{run},\gamma}$ denotes the running time of train p in block b', given a certain train driving strategy γ. Hence, the cumulative value of running time over $b' \in B_{p,b}$ is the trip time of train p

to the block b. $t_{p,b}^{\text{approach},\gamma}$ is the approach time of train p in block b with a certain train driving strategy γ. Additionally, $t_{p,b}^{\text{reaction}}$ is a constant parameter that represents the sight and reaction time before the braking indication point and $t_{p,b}^{\text{setup}}$ is the setup time of the route in the block that depends on whether the train is on open tracks or within the interlocking areas. For the latter, the $t_{p,b}^{\text{setup}}$ also depends on the number of switches involved in the route setting. While reaction time is a fixed parameter, and setup time is route-dependent, conservative values are chosen to account for stochastic variations, such as the communication delay of the Movement Authority from the Radio Block Centre to the train. As a result, Eq. (1) represents the Train Path Slot lower bound based on the nominal train driving with a scheduled departure and arrival time, while Eq. (2) hinges on the shifted MTTC driving strategy with a departure tolerance.

We use the shifted MTTC driving strategy to calculate the upper bound of the Train Path Slot $\bar{t}_{p,b}^{\text{TPS}}$. Besides, we add a fixed buffer time t_p^{buffer} after a train as part of the Train Path Slot upper bound. This increases the robustness of the train path since it could (partially) absorb the deviation of the preceding train from the scheduled trajectory and prevent delay propagation to the following train. The value of the buffer time could also be zero, depending on the timetable design. Without loss of generality, this buffer time can also be split into two parts, with one placed before the lower bound and the other after the upper bound. For ease of use in the following equations, we also provide the Train Path Slot upper bounds for the RMS and EETC driving strategies, which correspond to their respective blocking times without the additional buffer time.

$$\bar{t}_{p,b}^{\text{TPS}} = r_p + \sum_{b' \in B_{p,b}} t_{p,b'}^{\text{run},\gamma} + t_{p,b}^{\text{run},\gamma} + t_{p,b}^{\text{clear},\gamma} + t_{p,b}^{\text{release}} + t_p^{\text{buffer}}, \qquad \gamma = \text{MTTC}, \tag{4}$$

$$\bar{t}_{p,b}^{\text{TPS},\gamma} = \sum_{b' \in B_{p,b}} t_{p,b'}^{\text{run},\gamma} + t_{p,b}^{\text{run},\gamma} + t_{p,b}^{\text{clear},\gamma} + t_{p,b}^{\text{release}}, \qquad \gamma \in \{\text{RMS, EETC}\}, \tag{5}$$

where $t_{p,b}^{\text{run},\gamma}$ is the running time of train p in block b and $t_{p,b}^{\text{clear},\gamma}$ is the time for train p to clear the block b based on a specific train driving strategy γ. $t_{p,b}^{\text{release}}$ is a constant parameter to release the block b.

To represent the blocking time intervals allocated to a train across all blocks it traverses based on multiple driving strategies, we define the initial Train Path Slot TPS_p as a set of blocking time intervals, bounded by $\underline{t}_{p,b}^{\text{TPS}}$ from Eq. (3) and $\bar{t}_{p,b}^{\text{TPS}}$ from Eq. (4), respectively. This set defines a closed area in time–distance space, bounded by a piecewise constant lower and upper contour corresponding to the most extreme start and end times of the blocking times over successive blocks. This formulation extends the classical blocking time stairway representation by incorporating multiple train driving strategies, thereby capturing a range of possible blocking time intervals rather than a single deterministic trajectory. A visual representation of this concept is provided in Fig. 1, illustrating how the Train Path Slot defines the train's possible passage times over successive blocks. The formal definition of the initial Train Path Slot is given by:

$$\text{TPS}_p = \left\{ \left(b, \underline{t}_{p,b}^{\text{TPS}}, \bar{t}_{p,b}^{\text{TPS}}\right),\ b \in B_p \right\}. \tag{6}$$

3.3.3. Train Path Slot overlap detection

The conflict-free Train Path Slots of all concerned trains without overtaking must satisfy the following conditions:

$$\underline{t}_{p_j,b}^{\text{TPS}} \geq \bar{t}_{p_i,b}^{\text{TPS}} \quad \forall \left(p_i, p_j\right) \in P_2, b \in B_{p_i} \cap B_{p_j}, \tag{7}$$

where $\left(p_i, p_j\right)$ is a successive train pair in P_2. If an overtaking is scheduled, then the sequence of this train pair is reversed, which we will consider later.

The timetable planning tools of infrastructure managers usually have only target times as TP constraints at stations and/or important junctions. However, train trajectory uncertainty is not accounted for between these TPs and therefore, the Train Path Slots derived from the original timetable may have overlaps, i.e., Eq. (7) may not be met for all shared blocks with only the scheduled arrival times at arrival stations. Therefore, we check whether the upper bound of the preceding train p_i is conflicting with the lower bound of the following train p_j, similar to Bešinović et al. (2017). The Train Path Slot overlap $c_{p_i,p_j,b}$ between a successive train pair $\left(p_i, p_j\right)$ at the shared block b is computed as:

$$c_{p_i,p_j,b} = \max\left(0, \left(\bar{t}_{p_i,b}^{\text{TPS}} - \underline{t}_{p_j,b}^{\text{TPS}}\right)\alpha_{p_i,p_j,b} + \left(\bar{t}_{p_j,b}^{\text{TPS}} - \underline{t}_{p_i,b}^{\text{TPS}}\right)\left(1 - \alpha_{p_i,p_j,b}\right)\right) \quad \forall \left(p_i, p_j\right) \in P_2, b \in B_{p_i} \cap B_{p_j}, \tag{8}$$

where the binary parameter $\alpha_{p_i,p_j,b}$ equals 1 if train p_i precedes p_j at block b in the original order as specified in the given timetable while it equals 0 if the timetable indicates that train p_j precedes train p_i due to a scheduled overtaking before block b. If any $c_{p_i,p_j,b} > 0$, then a Train Path Slot overlap exists. Furthermore, we also consider partially parallel routes, such as on partial four-track lines or in stations where a planned overtaking occurs at scheduled stops. Let B_p^{parallel} represent the successive blocks of train p on a track of multiple-track line(s). On these blocks $b \in B_p^{\text{parallel}}$, the Train Path Slot overlaps should not be considered:

$$c_{p_i,p_j,b} = 0 \quad \forall \left(p_i, p_j\right) \in P_2, b \in \left(B_{p_i}^{\text{parallel}} \cup B_{p_j}^{\text{parallel}}\right) \setminus \left(B_{p_i}^{\text{parallel}} \cap B_{p_j}^{\text{parallel}}\right). \tag{9}$$

If no Train Path Slot overlap has been detected, the current TP configuration—with only target times at stations and/or important junctions—is sufficient to define the TPE and guide the train operation conflict-free. If an overlap is present, a Train Path Slot resolution module is required to optimise intermediate TPs, as detailed in the following subsection.

3.3.4. Train Path Slot overlap resolution

The resolution of Train Path Slot overlaps follows a two-step optimisation process. In the first stage, we formulate an LP model to determine conflict-free Train Path Slots by optimising their lower and upper bounds. The LP model contains two decision variables $x_{p,b}$ and $y_{p,b}$, representing the lower bound and the upper bound of the Train Path Slot in block b. However, since the LP model does not explicitly account for train dynamics, a second-stage sequential optimisation process is required to refine departure tolerances, determine intermediate TPs, and ensure operational feasibility, ultimately deriving the TPEs. For all successive train pairs $\left(p_i, p_j\right) \in P_2$, the LP model is formulated as Eqs. (10)–(14) in Box I where $\underline{t}_{p,b}^{\text{TPS}}$ and $\bar{t}_{p,b}^{\text{TPS}}$ are provided by the initial Train Path Slot lower and upper bounds.

For a railway corridor, the most flexible conflict-free Train Path Slots for all trains and all blocks they traverse can be found by maximising the terms in the first parentheses of Eq. (10), i.e., the difference between the upper and the lower bounds of the Train Path Slots. At the same time, if conflicts exist between a preceding and a following train, the terms in the second parentheses of Eq. (10) penalise differences between the optimised and initial lower bounds of the Train Path Slot to minimise impacts to nominal train operations. Essentially, the model primarily adjusts the upper bound of the initial Train Path Slot, which represents the robustness of the train path. This objective function collectively aims to fine-tune the departure tolerance for a preceding train, and only when no departure tolerance remains does it impose constraints on the nominal driving of the following train. In this way, the scheduled departure and arrival times from the real-time traffic plan are respected as much as possible.

Constraint (11) guarantees that the adjustments at overlapping shared blocks eliminate all Train Path Slot conflicts. No adjustment is needed if there is no overlap between a pair of successive Train Path Slots.

At any block section, the smallest blocking time is obtained when the train drives as fast as possible, namely by applying an MTTC driving

$$\text{Maximise} \sum_{p\in P}\sum_{b\in B_p}\left(y_{p,b}-x_{p,b}\right)+\left(\underline{t}^{\text{TPS}}_{p,b}-x_{p,b}\right)=\sum_{p\in P}\sum_{b\in B_p} y_{p,b}+\underline{t}^{\text{TPS}}_{p,b}-2x_{p,b}, \tag{10}$$

subject to

$$c_{p_i,p_j,b} \le \left[\left(\bar{t}^{\text{TPS}}_{p_i,b}-y_{p_i,b}\right)+\left(x_{p_j,b}-\underline{t}^{\text{TPS}}_{p_j,b}\right)\right]\alpha_{p_i,p_j,b} + \left[\left(\bar{t}^{\text{TPS}}_{p_j,b}-y_{p_j,b}\right)+\left(x_{p_i,b}-\underline{t}^{\text{TPS}}_{p_i,b}\right)\right]\left(1-\alpha_{p_i,p_j,b}\right) \quad \forall\left(p_i,p_j\right)\in P_2, b\in B_{p_i}\cap B_{p_j}, \tag{11}$$

$$y_{p,b}-x_{p,b} \ge \bar{t}^{\text{TPS}}_{p,b}-t^{\text{buffer}}_{p}-\underline{t}^{\text{TPS,MTTC}}_{p,b} \quad \forall p\in P, b\in B_p, \tag{12}$$

$$\underline{t}^{\text{TPS}}_{p,b} \le x_{p,b} \le \underline{t}^{\text{TPS,MTTC}}_{p,b} \quad \forall p\in P, b\in B_p, \tag{13}$$

$$\bar{t}^{\text{TPS},\gamma}_{p,b} \le y_{p,b} \le \bar{t}^{\text{TPS}}_{p,b} \quad \forall p\in P, b\in B_p, \gamma\in\{\text{RMS, EETC}\}, \tag{14}$$

Box I.

strategy. The right-hand side of constraint (12) represents this minimal blocking time, with the buffer time subtracted from the shifted MTTC to derive the plain MTTC upper bound. This constraint ensures that any optimised Train Path Slot will always accommodate at least the MTTC trajectory.

Constraints (13) and (14) provide the feasible solution space for the decision variables by considering the most critical driving strategy under nominal and delayed train operations. Specifically, the lower bound of a Train Path Slot must be smaller than the blocking time lower bound derived from the shifted MTTC strategy, while the upper bound must exceed the blocking time upper bound based on the slower of the RMS and EETC strategies.

The LP model provides an optimised, conflict-free set of Train Path Slots, which serves as constraints for subsequent response train trajectory generation. However, since the LP model does not fully capture train dynamics or give TPs, a further computation process is necessary. If the LP model fails to find a feasible solution, this indicates that the (re)scheduled timetable from the TMS contains conflicts that cannot be resolved by introducing additional TPs alone. In such cases, feedback is provided to the TMS, which must adjust the timetable to relax too restrictive headways between conflicting train pairs. Once the timetable is revised, the LP model is re-run in the next iteration to determine necessary TPs.

If the LP model finds a feasible solution, it produces three types of adapted slots as outputs:

1. Unchanged Train Path Slots: These remain intact as there is no overlap. A departure tolerance up to the running time supplement is available, and all three train driving strategies fit within these slots.
2. Adjusted upper bound: The upper bound of the initial Train Path Slot is modified, requiring a fine-tuned departure tolerance at the previous stop.
3. Adjusted lower and upper bounds: The Train Path Slot lower bound of the following train is modified, in addition to the Train Path Slot upper bound of the preceding train. In this case, the preceding train has no departure tolerance and must depart on schedule. The following train requires intermediate TPs with time constraints to resolve remaining Train Path Slot conflicts.

Therefore, the results from the LP model impose a set of Train Path Slot constraints on deriving the response train trajectories as follows:

$$\text{TPS}^{\text{cons}}_{p}=\left\{\left(b, x_{p,b}, y_{p,b}\right),\ b\in B_p\right\} \quad \forall p\in P. \tag{15}$$

According to the LP result, the departure tolerance is either zero (i.e., the train has to depart on time) or needs to be determined through an iterative process using the departure tolerance response driving strategy until the Train Path Slot constraint is satisfied. The departure tolerance response driving relies on an RMS driving strategy, where the train departs at the adjusted departure tolerance and uses the remaining running time supplement, computed as the difference between the scheduled supplement and the adjusted departure tolerance. Since blocking time overlap is used to fine-tune the departure tolerance, adjusting the running time supplement results in a different train trajectory, which in turn updates the blocking time. Thus, an iterative process is required. Each time, we compute the largest Train Path Slot overlap $c^{\max}_{p_i,p_j}$ of a successive train pair $\left(p_i,p_j\right)\in P_2$ in a chosen railway corridor as follows:

$$c^{\max}_{p_i,p_j}=\max_{b\in B_{p_i}\cap B_{p_j}}\left(c_{p_i,p_j,b}\right). \tag{16}$$

This maximum overlap is then used to update the departure tolerance:

$$\hat{\tau}^{\text{D}}_{p_i}\leftarrow\tau^{\text{D}}_{p_i}-c^{\max}_{p_i,p_j}, \tag{17}$$

where $\hat{\tau}^{\text{D}}_{p_i}$ is the restricted departure tolerance and $\tau^{\text{D}}_{p_i}$ is the departure tolerance from the last step, which corresponds to the initial departure tolerance in the first step. We present the iterative process described in Algorithm 1.

Algorithm 1 Description of fine-tuning departure tolerance.

Input: Inputs to the modelling framework, the largest Train Path Slot overlap $c^{\max}$, initial departure tolerance τ^{D}_{p} and Train Path Slot constraint $\text{TPS}^{\text{cons}}_{p}$
Output: Restricted Train Path Slot, fine-tuned departure tolerance $\hat{\tau}^{\text{D}}_{p}$
while $c^{\max}>0$ **do**
  Step 1 Update departure tolerance: $\hat{\tau}^{\text{D}}_{p}=\tau^{\text{D}}_{p}-c^{\max}$
  Step 2 Calculate departure tolerance RMS response train trajectory for $\hat{\tau}^{\text{D}}_{p}$ to the next scheduled arrival stop
  Step 3 Compute the updated Train Path Slot upper bound $\bar{t}^{\text{TPS,RMS}}_{p,b}$ at each block b that train p traverses
  Step 4 Set the new largest Train Path Slot overlap: $c^{\max}=\max_{b\in B_p}\left(\bar{t}^{\text{TPS,RMS}}_{p,b}-y_{p,b}\right)$
  Step 5 Update the initial departure tolerance: $\tau^{\text{D}}_{p}=\hat{\tau}^{\text{D}}_{p}$
end while

We present a time–distance diagram as an example to explain the update of the departure tolerance in Fig. 4, which corresponds to the second type of adapted slot from the LP model. As shown in the left part of the figure, the initial departure tolerance of the preceding train leads to five Train Path Slot overlaps with the following train. To resolve these conflicts, the largest Train Path Slot overlap is iteratively identified and used to adjust the departure tolerance until a feasible value is found that eliminates all overlaps. Since the departure tolerance response strategy maintains the same total running time supplement, the remaining supplement is given by the initial supplement minus the adjusted departure tolerance. This fine-tuning process leads to a

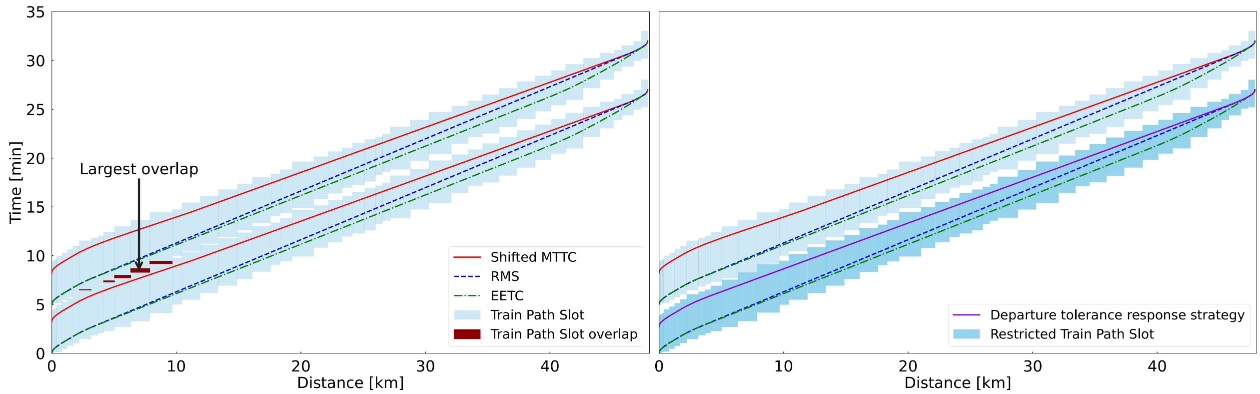

Fig. 4. Time–distance diagram example of initial conflicting Train Path Slots (left) and optimised Train Path Slots after fine-tuning departure tolerance for the preceding train (right).

restricted Train Path Slot that meets the Train Path Slot constraint as the right part of the figure displays.

The third type of adapted Train Path Slots from the LP model necessitates one or more intermediate TP $s \in S_p$ in case the fine-tuned departure tolerances cannot resolve all the Train Path Slot overlaps. These intermediate TPs are located at the beginning of a block $b \in B_p$ such that the Train Path Slot constraint can be respected. Introducing intermediate TPs triggers a TP response driving strategy that considers the train dynamics and consequently modifies the blocking times. Therefore, each time an intermediate TP is defined, the Train Path Slots must be updated and re-evaluated to determine whether the overlap is resolved or if additional intermediate TPs are required.

We propose a *critical-block TP configuration*, where an intermediate TP is added to the set S_{p_j} for the following train p_j in a successive train pair $(p_i, p_j) \in P_2$ at the beginning of the critical block, namely the block with the largest Train Path Slot overlap. Specifically, we add the intermediate TP among all possible TP locations $s_b \in S'_{p_j}$ where the value of the Train Path Slot overlap is maximised:

$$s = s_b \text{ with } b = \underset{b \in B_{p_j}}{\operatorname{argmax}} \left(c_{p_i,p_j,b} \mid (p_i, p_j) \in P_2 \right). \tag{18}$$

This TP configuration imposes the most restrictive constraint on train trajectory generation by considering the tightest headway between two trains to ensure conflict-free operations. The concept of the critical block is also used in the International Union of Railways (UIC) timetable compression method to determine the minimum line headway time between two successive trains in (re)scheduling (Goverde et al., 2013; UIC, 2013). However, unlike in timetable compression, where headway times are computed based on single train trajectories, the blocking times here are directly influenced by the fixed scheduled headways from the timetable and the introduction of a TP at the critical block. Since the Train Path Slots account for a range of possible train trajectories, an iterative process is required to adjust train trajectories to fit the requested headways, identify new critical blocks, and introduce additional TPs where necessary.

The TP response strategy combines RMS and EETC driving strategies, using multiple response cruising speeds to meet the Train Path Slot constraints while including a coasting regime between the last intermediate TP and the next stop. First, we consider the previous stop with the scheduled departure time as a starting TP and use the prescribed intermediate TP at the critical block as an endpoint. Aiming for the maximum time window at the intermediate TP, we apply the Golden-section search to find the largest response cruising speed up to the defined intermediate TP. The search terminates once the Train Path Slot constraints at the critical block are met, or there exists only a sufficient buffer time between two trains. If Train Path Slot overlaps persist, additional intermediate TPs are introduced at the next most critical locations. Depending on whether the newly added intermediate TP is upstream or downstream of the previous one, the starting and endpoint of the response trajectory are updated accordingly to determine an optimal response cruising speed. When more than one intermediate TP is defined, maximum traction and service braking are applied to transition between different response cruising speeds. Once all Train Path Slot constraints are satisfied, we refine the response cruising speed between intermediate TPs (if more than one) for the maximum time window. Finally, we compute an energy-efficient train trajectory between the last intermediate TP and the next stop. Depending on the remaining running time supplement, the train either accelerates to an optimal cruising speed before coasting or transitions directly into coasting from the last cruising speed. As the running time supplement is reallocated between stops through intermediate TPs, the train progresses later in its trajectory and ensures sufficient buffer time for the successive train pair after the last intermediate TP.

3.3.5. *Train Path Envelope computation with optimised timing points*

The final module integrates both stages of Train Path Slot overlap resolution and assembles the optimised TPs with either time windows or target times into TPEs, facilitating conflict-free train operations. The locations and the temporal constraints of the TPs depend on the results from the Train Path Slot overlap detection and resolution modules. Hence, the set of TPs S_p for a train $p \in P$ could be at stop locations or the beginning of blocks where constraints must be imposed to train trajectory generation. We formulate the TPE as an ordered set of TP constraints as follows:

$$\text{TPE}_p = \left\{ \left(s, t^{\min}_{p,s}, t^{\max}_{p,s} \right),\ s \in S_p \right\} \quad \forall p \in P, \tag{19}$$

where $t^{\min}_{p,s}$ and $t^{\max}_{p,s}$ represent the lower and upper bounds of the departure or passing time window at the TP s based on the driving strategies that define the contours of a conflict-free Train Path Slot. The lower bound of a time window $t^{\min}_{p,s}$ denotes either the passing time of the TP response strategy at an intermediate TP or the scheduled departure time at a stop. The upper bound of a time window $t^{\max}_{p,s}$ corresponds to either the passing time of the shifted MTTC or the departure tolerance response driving strategy at an intermediate TP or the departure tolerance at a stop. If a TP specifies a fixed time (e.g., a scheduled arrival time at a stop), then the time window becomes a target time by having $t^{\min}_{p,s} = t^{\max}_{p,s}$.

We visualise the target time and the time window as two types of TP constraints in Fig. 5. The left-hand side of Fig. 5 represents a train run between two stops and has only one target arrival time at the next stop. In contrast, the right-hand side of Fig. 5 is a restricted Train Path Slot that includes a fine-tuned departure tolerance at the previous station (0 m) and an intermediate passing time window at 26,000 m.

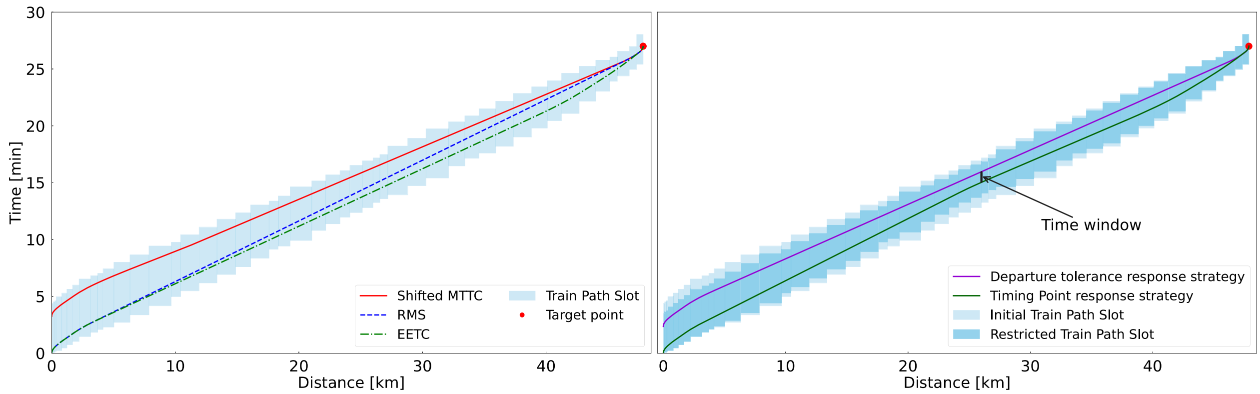

Fig. 5. Time–distance diagram example of an initial Train Path Slot with just the target time (left) and an optimised Train Path Slot with both target time and time window at Timing Points (right).

3.4. Evaluation criteria

3.4.1. Alternative timing point configurations

To assess the effectiveness of the proposed *critical-block TP configuration*, we compare it against two other alternative approaches: the *scheduled TP configuration* and *earliest-conflict TP configuration*. The *scheduled TP configuration* represents the current practice, where only scheduled target departure and arrival times at stops are provided. On the other hand, the *earliest-conflict TP configuration* introduces an intermediate TP to the set S_{p_j} for the following train p_j at the beginning of the first conflicting block. In detail, this TP is placed at the entry location of the block with the lowest topological order among all conflicting blocks where the Train Path Slot overlap is positive:

$$s = s_b \text{ with } b = \operatorname*{argmin}_{b \in B_{p_j}} \left(c_{p_i, p_j, b} \mid (p_i, p_j) \in P_2 \right). \tag{20}$$

3.4.2. Key performance indicators

The performance of different TP configurations can be quantified by several Key Performance Indicators (KPIs), considering both timetable-level and train operation-level metrics. From the timetable perspective, the Train Path Slot overlaps under a specific TP configuration are assessed, for instance, those occurring under the *scheduled TP configuration*. Additionally, the infrastructure occupation is quantified based on the UIC timetable compression method (UIC, 2013). From a train operation perspective, we consider the number of added intermediate TPs since this affects the efficiency of the onboard train trajectory generation and the quality thereof, particularly, energy efficiency. We calculate the energy consumption based on the train control problem using the mass-specific applied force and the total distance. Moreover, the number of added intermediate TPs also leads to a different number of possible braking indication points and driving regime changes, both of which have implications for passenger comfort. Note that the number of braking indication points refers to the deceleration action of the ATO onboard to avoid triggering emergency braking because of conflicting block sections. The above concepts are captured in several performance indicators as follows:

- *Train Path Slot overlap time*: The total Train Path Slot conflicting time over the entire railway corridor (in seconds).
- *Infrastructure occupation*: The share of time a given timetable pattern occupies a given infrastructure in an hour (in percentage).
- *Added intermediate Timing Points*: The number of added intermediate Timing Points to resolve the Train Path Slot overlaps.
- *Energy consumption*: The amount of energy consumed by the train operation (in kWh).
- *Braking indications points*: The number of braking indication points to prevent onboard emergency brake intervention.
- *Driving regime changes*: The number of driving regime switches in the computed train trajectory. For instance, the train driving shifting from cruising to braking is counted as one time.

4. Analysis and results

This section first presents the model verification with 16 scenarios in Section 4.1, demonstrating the effectiveness of fine-tuning departure tolerances and introducing critical-block TPs. The methodology is then applied to a real-world case study in Section 4.2, followed by a detailed performance evaluation in Section 4.3. Finally, Section 4.4 assesses the system improvements achieved by the proposed method.

All computational experiments are conducted on a laptop with an Intel(R) Core(TM) i7-10610U CPU (1.80 GHz) and 16 GB RAM. The LP model for conflict-free Train Path Slot determination is solved to optimality using PuLP, an open-source Python optimisation library, which employs the Revised Simplex Method by default to solve the LP problem. Train trajectory generations are solved using a numerical approach based on train dynamics and optimal control principles. The LP model execution time is typically under 0.1 s, while trajectory computation varies depending on the number of calculations and intermediate TPs required.

4.1. Model verification

The proposed method for determining an optimised set of TPs is verified in an experimental setup with 16 scenarios of different train pairs. These scenarios assess the effectiveness of fine-tuning the departure tolerance and the critical-block TP strategy. A 21.5 km route is defined, consisting of 17 block sections and 2 intermediate stations with varying gradients and speed limits. The first and second intermediate stations are 10,187 m and 15,092 m from the origin station, respectively. Both Intercity and Regional trains are operated on this test case with a maximum speed of 140 km/h. The scenarios vary by train order, stopping patterns, and train types. Specifically, an Intercity train may or may not stop at the first intermediate station, while a Regional train may stop at the second intermediate station, both stations, or neither. The service braking rates of Intercity and Regional trains are $-0.8\ \mathrm{m/s^2}$ and $-0.66\ \mathrm{m/s^2}$, respectively. These values are based on the operational braking characteristics of Dutch passenger trains and are consistent with those used in previous train trajectory optimisation studies. Since only braking rate data was available to describe braking behaviour, the braking force is calculated as the product of braking rate and train mass, plus resistance forces. For a more detailed description of the basic train characteristics used, see Goverde et al. (2021). The blocking time-related parameters in Eqs. (1)–(2) and (4)–(5) are set from ETCS Level 2 characteristics and consider the potential influence of ATO, following consultation with the Dutch railway infrastructure

Table 3
Computational results for all scenarios.

Scenario	Preceding train (# stops)	Following train (# stops)	Headway (s)	Train path slot overlap (s)	Departure tolerance at stops (s)	Timing Point locations (m)	Block index	Time windows (s)	Computation time (s)
1	Intercity (0)	Intercity (0)	210	80	45	–	–	–	6
2	Intercity (0)	Intercity (0)	180	110	0	14 248	block 12	71	7
3	Intercity (0)	Intercity (1)	216	74	78	–	–	–	2
4	Intercity (0)	Intercity (1)	132	158	0	3664, 1929	Block 5, block 4	60, 76	12
5	Intercity (1)	Intercity (0)	480	39	Full, 48	–	–	–	4
6	Intercity (1)	Intercity (0)	318	81	Full, 0	14 248	Block 12	82	4
7	Regional (0)	Regional (0)	240	76	77	–	–	–	2
8	Regional (0)	Regional (0)	174	142	0	12 471	Block 11	89	7
9	Regional (0)	Regional (1)	222	94	57	–	–	–	4
10	Regional (0)	Regional (1)	156	160	0	1929	Block 4	108	6
11	Regional (1)	Regional (0)	276	40	Full, 12	–	–	–	4
12	Regional (1)	Regional (0)	258	58	97, 0	16 027	Block 14	66	10
13	Regional (1)	Intercity (0)	330	26	Full, 28	–	–	–	2
14	Regional (1)	Intercity (0)	300	56	Full, 0	16 027	Block 14	76	4
15	Regional (2)	Intercity (0)	420	37	Full, full, 13	–	–	–	2
16	Regional (2)	Intercity (0)	396	61	Full, full, 0	14 248	Block 12	95	6

manager, ProRail. Specifically, the values are set as follows: $t_{p,b}^{\text{release}} = 2$ s, $t_{p}^{\text{buffer}} = 30$ s, $t_{p,b}^{\text{reaction}} = 1$ s, and $t_{p,b}^{\text{setup}} = 1$ s for open track. In station areas or junctions, the setup time is defined as $t_{p,b}^{\text{setup}} = 6 \times$ number of switches (in seconds). For ETCS Level 2, the setup time may also include additional processing and communication delays. The 30 s buffer time accounts for these variations and provides sufficient margin for longer setup times when required. The parameter values can be adjusted when better estimates are available without impact on the method. In this test case, the intermediate stations are actual stations with switches.

Table 3 presents the computational results for the 16 scenarios, reporting the stop pattern and the train type of both the preceding and following trains, their headway, Train Path Slot overlaps, fine-tuned departure tolerance at stops of the preceding train, intermediate TP locations of the following train, corresponding block indices, time windows at these intermediate TPs, and total computation time for each scenario. The headway values in Table 3 are systematically selected to evaluate the effectiveness of the proposed method for TP optimisation under varying traffic conditions. These values distinguish cases where departure tolerances can be fine-tuned to resolve blocking time conflicts from those that require intermediate TPs. For excessively tight headways, the TPE generation module warns the TMS that no feasible conflict-free solution exists. For a certain train pair, we first only utilise fine-tuning departure tolerance of the preceding train to avoid Train Path Slot overlaps. Then, we illustrate the usefulness of determining intermediate TPs for the following train when the headway is shortened and no departure tolerance at the previous stop is allowed. For scenarios where the preceding train makes multiple stops, multiple values for departure tolerances are displayed. Similarly, when multiple intermediate TPs are required, their locations and time windows are reported accordingly.

If the departure tolerance fine-tuning cannot fully resolve the Train Path Slot overlaps, intermediate TPs at the entry locations of the most critical blocks provide a further means of resolving overlaps, provided a feasible solution space exists. The results indicate that, in most cases, a single intermediate TP suffices. However, in scenario 4, a lower response cruising speed imposed by an intermediate TP at block 5 successfully resolves the conflict at that location but causes a new overlap at block 4. In such cases, an additional intermediate TP is necessary at the updated most critical block to ensure conflict-free train operations.

For each scenario of a train pair, we observe that the computation time increases when fine-tuning the departure tolerance cannot fully resolve the Train Path Slot overlaps and intermediate TPs are needed with additional calculations. Among the computational steps, generating the TP response train trajectory demands the most computational time. On the one hand, 2 to 6 s are required to resolve the Train Path Slot overlaps by fine-tuning the departure tolerances, depending on the number of iterations needed to address the largest overlap in each step. On the other hand, the computation time for determining a feasible TP response train trajectory ranges from 2 to 12 s, depending on the number of intermediate TPs introduced. This variation is due to the need to iteratively determine response cruising speeds that satisfy the Train Path Slot constraints.

The results further show that the placement of intermediate TPs is influenced by the characteristics of train operations. In homogeneous traffic conditions, the intermediate TP is added mostly halfway between two stops because the energy-efficient train driving deviates gradually from the scheduled train path and the buffer in the timetable is insufficient to absorb this deviation. If the preceding train has multiple stops, the intermediate TPs are mainly specified for the following train after the last stop of the preceding train, where the following train is likely to approach the preceding one. Reversely, if the following train has multiple stops, the intermediate TPs are usually given in the first part of the journey, where the headway is tight. We visualise two examples of the 16 scenarios in Fig. 6 with scenarios 4 and 12.

4.2. Case study description

Our case study takes place on one of the busiest railway traffic corridors in the Netherlands between Utrecht and ’s-Hertogenbosch. This fifty-kilometre-long railway corridor includes nine passenger stations: Utrecht (Ut), Utrecht Vaartsche Rijn (Utvr), Utrecht Lunetten (Utln), Houten (Htn), Houten Castellum (Htnc), Culemborg (Cl), Geldermalsen (Gdm), Zaltbommel (Zbm) and ’s-Hertogenbosch (Ht). In particular, the Ut-Htnc railway is four-track, and station Gdm has 7 tracks, which permits overtaking. The rest is double-track (one track per direction). We use the periodic timetable of 2022 for the case study corridor (single direction from Ut to Ht). The railway timetable repeats itself every half-hour, featuring three Intercity and three Sprinter (i.e., regional) services per cycle. Nevertheless, the departure intervals of trains are not regular in this alternative Intercity/Sprinter periodic timetable due to the need to plan freight train paths and other constraints (e.g., the arrival of the same rolling stock from the opposite direction or infrastructure limitations). The Intercity stops at the two corridor ends, while the Sprinter stops at every station. As the trains from different directions are independent of each other, we only consider the trains from Ut to Ht within each 30 min cycle.

The train parameters (e.g., maximum speed, braking rates, and acceleration characteristics) and fixed blocking time components (e.g., reaction times, release times) are consistent with the model verification subsection. Additionally, the speed limit and gradient profile information can be inferred from the speed profile presented in the following subsections. The infrastructure occupation is 62.11% (corresponding to a compressed timetable of 1118 s in 1800 s), calculated following

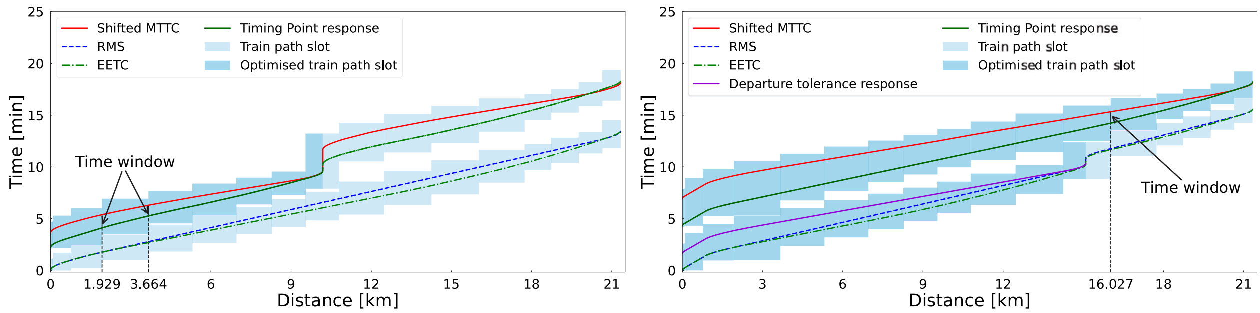

(a) Scenario 4 (b) Scenario 12

Fig. 6. Optimised Train Path Slots for scenarios 4 and 12.

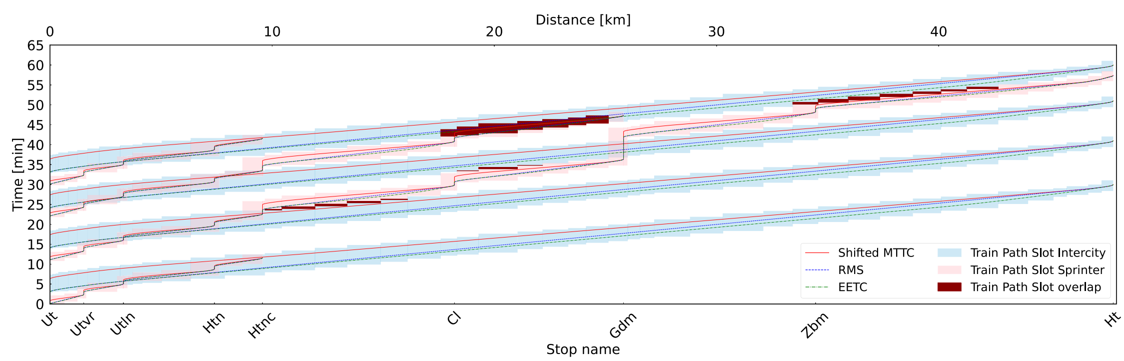

Fig. 7. Train Path Slots for the original timetable.

the compression method of the UIC 406 method and the blocking time stairways based on the RMS driving strategy. This is in line with the usual timetable planning approach of infrastructure managers. Note that infrastructure occupation is computed from the first train in a half-hour cycle to the same train in the next cycle. The infrastructure occupation value is below the recommended value of 75% during peak periods for mixed-traffic corridors.

4.3. Results

We start by analysing the Train Path Slots for the case study, as illustrated in Fig. 7. Generally, the EETC-based train paths occur earlier than the RMS-based ones since the optimal cruising speed is usually higher to allow coasting at a later stage, causing variations in train paths between stops, as only scheduled train event times at stops are specified in the timetable. As a first robustness check and initial Train Path Slot computation, the initial Train Path Slots are calculated using the full departure tolerances, which results in Train Path Slot overlaps. These overlaps indicate potential train path conflicts and serve as input to the LP model, after which departure tolerances are fine-tuned. In total, four Train Path Slot overlaps are detected after the departure of Sprinter trains from stations Htnc, Cl, and Zbm, with a cumulative overlap duration of 1352 s.

The proposed LP model is then applied to determine conflict-free Train Path Slots and identify the necessary TP configuration for each train. As shown in Fig. 8, no Train Path Slot constraints are required for the first Sprinter and third Intercity. Hence, the departure time windows for these trains remain equal to the running time supplement, and the scheduled arrival times at stops correspond to their TP configurations in the TPEs. However, departure tolerance adjustments are required for the second Intercity and second Sprinter at station Cl. Furthermore, the departure tolerance is set to zero for the second Sprinter at station Zbm and the third Sprinter at station Cl. Lastly, intermediate TPs must be introduced for the fourth Intercity train, i.e., the first train in a half-hourly periodic timetable.

Building upon the conflict-free Train Path Slots determined by the LP model, the proposed *critical-block TP configuration* fine-tunes departure tolerances and introduces intermediate TPs at the critical blocks. After applying the fine-tuning departure tolerance algorithm, the departure tolerance of the second Intercity is shortened by 50 s (from 195 s to 145 s) to resolve the Train Path Slot overlaps after the departure of the second Sprinter at station Htnc. For the second Sprinter, its departure tolerance at station Cl is reduced by 37 s (from 76 s to 39 s), and a scheduled departure time is imposed at station Zbm (zero departure tolerance). The third Sprinter also has zero departure tolerance at station Cl. Even with zero departure tolerance, a buffer time of 30 s is still available to accommodate small departure delays. To resolve the remaining overlaps, an intermediate TP is placed at the start of the last block before station Gdm for the fourth Intercity. This TP is positioned at the most restrictive block, ensuring that all residual conflicts are eliminated. This location of the critical block has been validated against real-life track occupation data provided by the Dutch railway infrastructure manager, ProRail. The results confirm that the conflict detected before station Gdm is observed in 46% of the operated daily schedule in real-world operations.

The TP response strategy uses almost all the running time supplement to meet the Train Path Slot constraint with approximately 13 s left as the running time supplement for the rest of the journey. The TP response driving strategy avoids any extra braking. The train performs one additional acceleration regime after the newly introduced TP and then attains another cruising speed followed by coasting and braking before reaching the next stop, as shown in Fig. 9. Beyond this intermediate TP, no further intermediate TPs are required after station Zbm. This is because the train compensates for its adjusted trajectory by spending additional time in the section between station Ut and the intermediate TP, meeting all Train Path Slot constraints. Hence, the

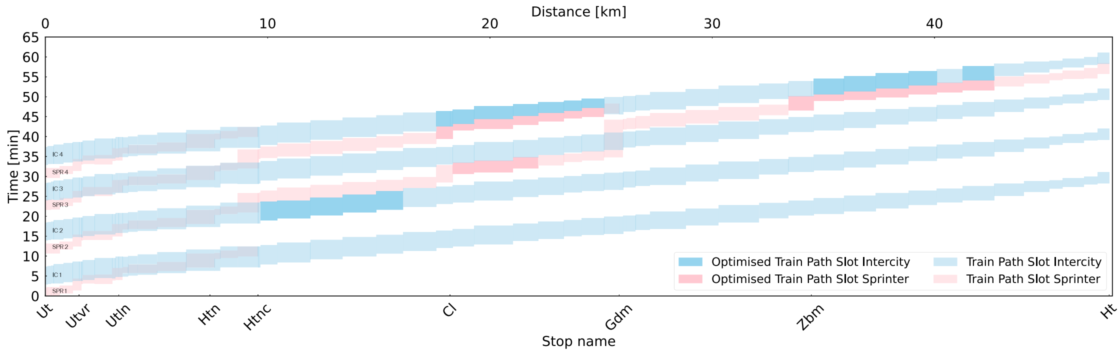

Fig. 8. Optimised Train Path Slots based on the Linear Programming model.

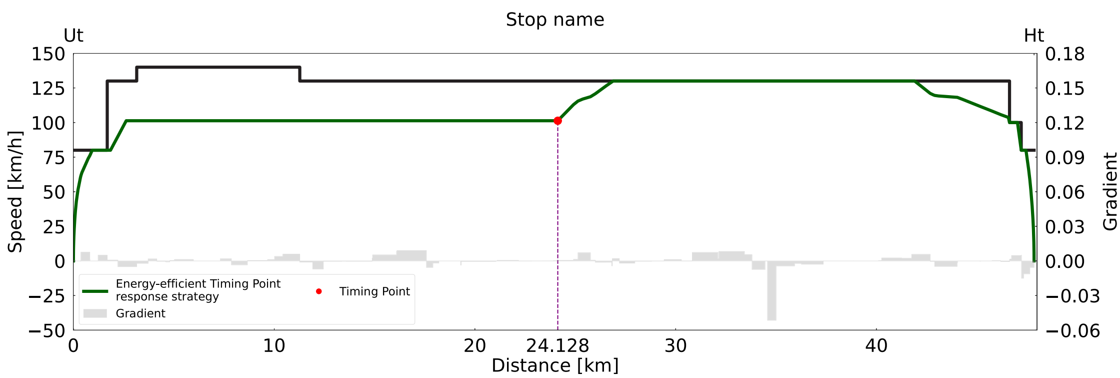

Fig. 9. Timing Point response speed profile of the conflicted train for the critical-block Timing Point configuration.

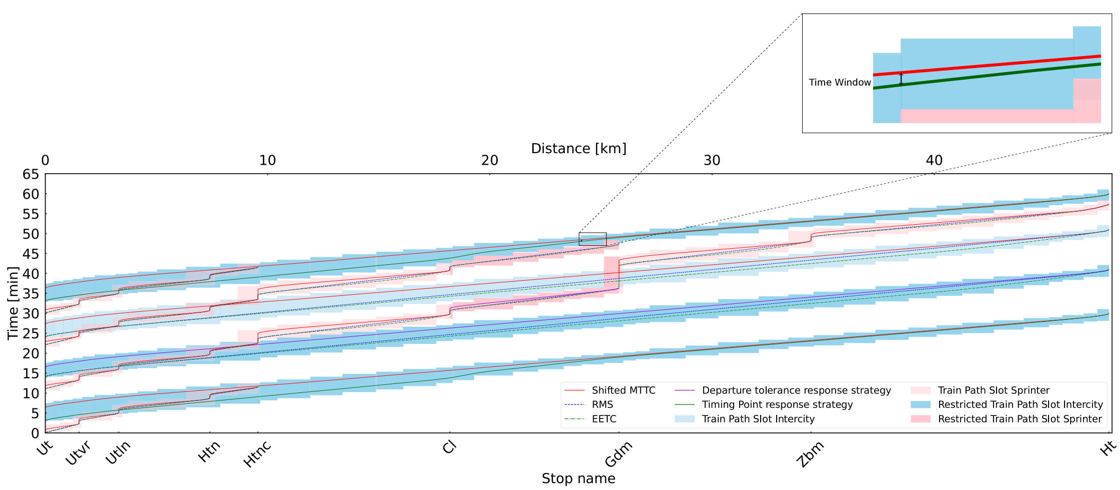

Fig. 10. Train Path Slots with the critical-block Timing Point configuration.

departure tolerance for the conflicted Sprinter train can be fine-tuned again, as illustrated in Fig. 10.

The total computation time of the optimised ATO TPs for a given timetable depends on the corridor length, the number of conflicting train pairs and the number of intermediate TPs required. It takes around 11 s to generate the initial Train Path Slots for all trains in the case study, including blocking time computation for the given three train trajectories per train, shared track identification, and visualisation of the initial Train Path Slots with departure times added, excluding the pre-computed train trajectories used to build the slots. The LP model execution time is 0.1 s, while fine-tuning the departure tolerances of all conflicted trains takes around 12 s. Determining the time window for the critical-block TP configuration needs approximately 6 s to determine the optimal cruising speed of the response speed profile before the intermediate TP. In total, the computation time for the entire case study, involving eight trains with an average departure headway of 5 min, is 29 s.

4.4. System improvement

To evaluate the system improvement achieved by the proposed *critical-block TP configuration*, we compare its performance with two benchmark cases: the *scheduled TP configuration* and the *earliest-conflict TP configuration*. The *scheduled TP configuration* represents the current practice, where TPs are placed only at scheduled stops. However, as the optimisation results indicate, relying solely on restrictive scheduled departure time windows cannot fully resolve Train Path Slot overlaps,

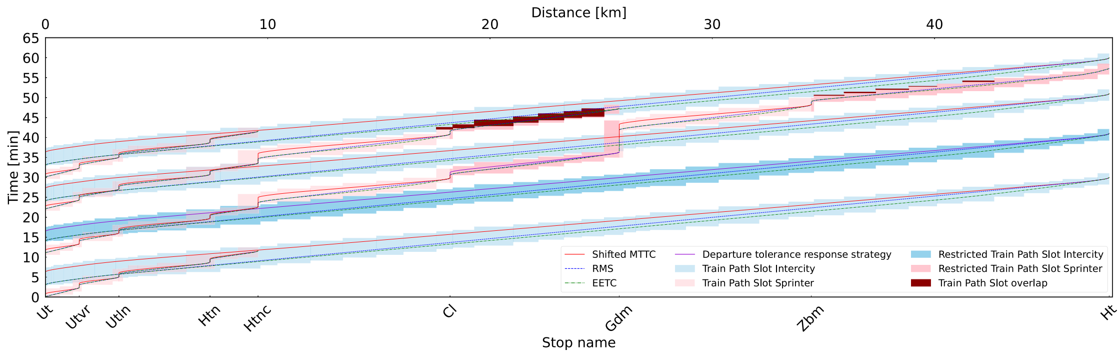

Fig. 11. Train Path Slots with the scheduled Timing Point configuration.

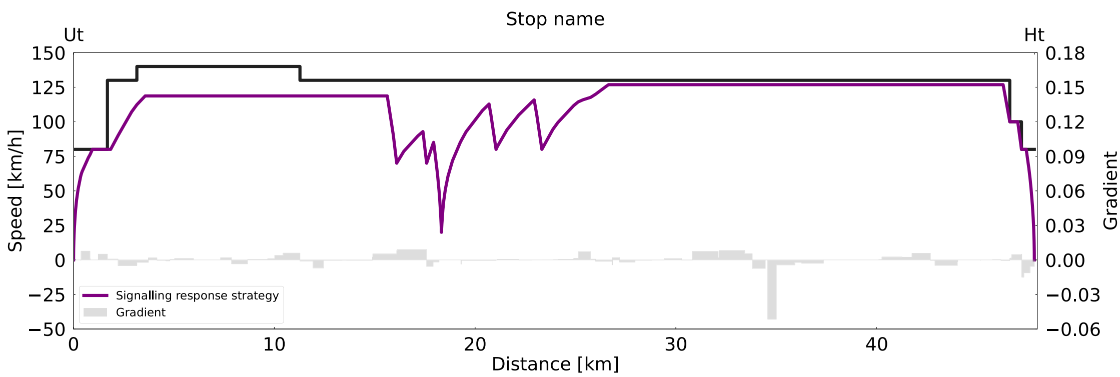

Fig. 12. Signalling response speed profile of the conflicted train for the scheduled Timing Point configuration.

which equals to 623 s between the second and third Sprinters and the fourth Intercity, as shown in Fig. 11.

Without adding intermediate TPs, the fourth Intercity must react to the signalling system. Before reaching conflicting block sections, it follows the optimal cruising speed based on the EETC driving strategy. However, its ATO onboard system then issues a speed reduction command, keeping the train below the braking curve computed by the ETCS onboard system before reaching the conflicting block. The train decelerates accordingly to avoid triggering emergency braking and re-accelerates as soon as its rear has passed the speed reduction section. Yet, this acceleration may trigger another braking curve, as the speed increase could again conflict with the block occupation by the preceding train. The incapability of anticipating the upcoming signals in real-time can lead to a zig-zag movement, as shown in Fig. 12. Compared to nominal EETC-based operation (without train path conflicts), this Intercity needs to comply with five extra braking indication points and undergoes ten driving regime changes within the Train Path Slot overlapping area. After the conflict area, only 14 s of running time supplement remain, leading the train to adopt an optimised cruising speed below the speed limit to arrive at the next stop punctually. This inefficient response increases energy consumption by 177.99 kWh, representing a 53.2% increase compared to the 334.63 kWh required under nominal EETC operation. The realised infrastructure occupation time is 2455 s per hour, resulting in a 9.79% increase in infrastructure occupation ratio, reaching 68.19%, considering the signalling response driving strategy of the fourth Intercity and the EETC driving strategy for the other trains. In contrast, the *critical-block TP configuration* increases infrastructure occupation time to 2495 s per hour, resulting in an 11.59% increase in infrastructure occupation ratio compared to the baseline of 62.11%, which rises to 69.31%. However, its TP response driving strategy substantially improves energy efficiency, reducing consumption by 152.53 kWh, a 29.75% decrease compared to the signalling response strategy.

Another benchmark, the *earliest-conflict TP configuration*, fine-tunes departure tolerances and introduces intermediate TPs, starting from the first conflicting block. After an iterative process to meet the conflict-free Train Path Slot constraints from the optimisation model, six additional TPs are required for the fourth Intercity, with the last one corresponding to the critical block TP. The first TP is provided at the beginning of the block before station Cl, while the second and the third TPs are placed at the start of the following two blocks since the Train Path Slot overlap gradually increases across these sections. The same pattern is also seen for the fourth, fifth and sixth TPs, positioned at the start of the last three blocks before station Gdm. Therefore, a larger Train Path Slot overlap in downstream blocks imposes more restrictive constraints for the train trajectory computation, which requires additional TPs to ensure conflict-free operations. Since the LP model aims to maximise flexibility in blocking time windows, the time windows at intermediate TPs also strive to be as large as possible. To assess sensitivity, we also tested decreasing the window size for the first intermediate TP to make it more restrictive, which resulted in a lower total number of required TPs. However, the TP at the critical block remains essential to achieving effective conflict-free train operations with the given running time supplement. This result reinforces the rationale for adopting the *critical-block TP configuration*. Compared to the signalling response strategy, the TP response strategy for the *earliest-conflict TP configuration* reduces energy consumption by 96.75 kWh (18.87%), requires two fewer braking indication points and results in two fewer driving regime changes. We present the realised Train Path Slots for the earliest-conflict TP configuration in Fig. 13.

We report the results of the three TP configurations in Table 4, using the selected KPIs to compare their impact on system performance. In this table, columns regarding added intermediate TPs, energy consumption, extra braking indication points, and extra driving regime changes are quantified based on either the signalling response driving strategy or the TP response strategy of the conflicted train. Extra braking indication points and driving regime changes are benchmarked

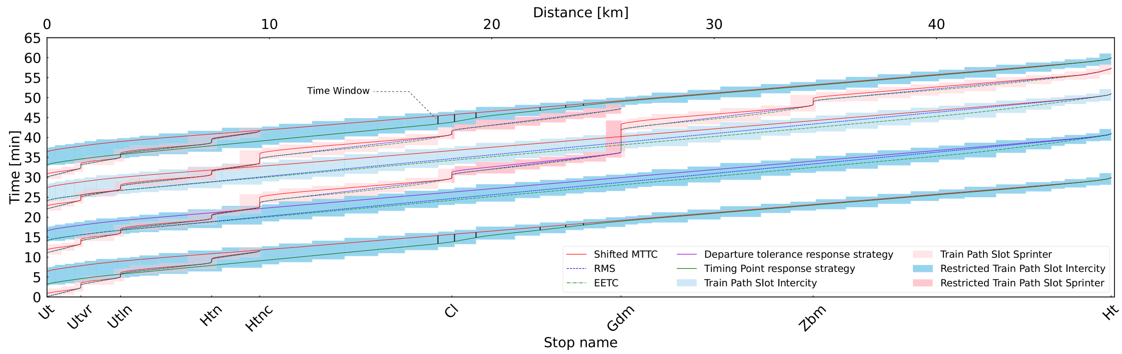

Fig. 13. Train Path Slots with the earliest-conflict Timing Point configuration.

Table 4
The results of different Timing Point configurations.

	Figure	Slot overlap time [s]	Infrastructure occupation [%]	Added intermediate Timing Points	Energy consumption [kWh]	Extra braking indication points	Extra driving regime changes
Critical-block Timing Point configuration	10	0	69.31%	1	360.09	0	1
Scheduled Timing Point configuration	11	623	68.19%	0	512.62	5	10
Earliest-conflict timing point configuration	13	0	69.31%	6	415.87	3	8

against the nominal EETC train driving strategy. The *scheduled TP configuration*, representing current practice, demonstrates that TPs at scheduled stops are insufficient, as they fail to resolve the Train Path Slot overlaps. Without intermediate TPs, conflicts persist, leading to inefficient train operations with frequent braking interventions and increased energy consumption. This highlights the necessity of optimising TP configuration to ensure conflict-free train operations.

In contrast, both the *earliest-conflict* and *critical-block TP configurations* eliminate Train Path Slot overlaps and improve operational efficiency. However, the *earliest-conflict TP configuration* requires six additional TPs to achieve conflict-free operations, introducing multiple constraints that restrict train trajectory generation and tracking flexibility. While it resolves conflicts, it also leads to higher energy consumption and frequent braking interventions as the train must comply with multiple intermediate TPs across its journey. The *critical-block TP configuration* ensures conflict-free operations without imposing excessive trajectory constraints by introducing a single TP at the most restrictive block. Compared to the *earliest-conflict* TP configuration, it significantly reduces energy consumption, braking interventions, and driving regime changes, while maintaining the same infrastructure occupation efficiency. As a result, the *critical-block TP configuration* proves to be the most effective approach, outperforming the alternatives across almost all KPIs.

5. Discussion

The proposed method for optimising TPs in TPEs provides practical decision-making benefits for railway infrastructure managers, undertakings, and ongoing standardisation efforts, such as those within the European Rail Traffic Management System (ERTMS) and ATO development. This method establishes a structured interface between traffic management and train operations, ensuring a decoupling of trackside and onboard functions for conflict-free train operations while maintaining driving flexibility. This TPE computation can function as an independent module, either within an ATO trackside or as part of the TMS.

This study advances the formalisation of open issues within ERTMS/ATO, particularly in the requirements specification between TMS and ATO trackside (UNISIG, 2023), where TP granularity remains undefined for effectively guiding ATO. The proposed critical-block TP configuration introduces a systematic approach to this process, which ensures conflict-free train operations without necessitating major modifications to the existing system architecture. This approach improves traffic fluidity while preserving operational flexibility for railway undertakings and offers a cost-effective alternative to capacity expansion. These findings align with the objectives of Europe's Rail FP1-MOTIONAL project, which aims to enhance traffic management and integrate digital solutions for more resilient and optimised rail operations.

The method applies to both vertically integrated and separated railway structures, aligning timetable-based traffic management with speed-based train operations. Traditional timetable (re)scheduling approaches assume deterministic train trajectories, whereas real-time train operations introduce variability due to different driving strategies and other operational conditions. The proposed Train Path Slot concept bridges this gap by considering multiple driving strategies and incorporating buffer time to accommodate operational uncertainties.

Beyond train path conflict resolution, the model improves train path robustness and energy efficiency. Fine-tuned departure tolerances establish a structured upper bound on allowable departure delays and, therefore, on the latest possible train running time, which enhances the tractability of conflict detection algorithms and the adaptability of train operations. By strategically adjusting TP locations and departure tolerances, trains proactively optimise their trajectories based on the determined TPs and reduce unnecessary driving regime transitions. This approach enables a network-wide green wave, where trains operate at optimised speeds under given headways from the real-time traffic plan without unneeded slowdowns due to restrictive signalling. Once the real-time traffic plan is updated, automated TPE optimisation streamlines downstream train operations, which is applicable in both human-supervised and automated TMS environments.

While the proposed method optimises TP configurations and generates conflict-free TPEs, certain limitations remain that may affect its scalability and real-time applicability. First, computational efficiency poses challenges for large-scale real-world implementations. Although the LP-based optimisation efficiently resolves conflicts, repeated multiple train trajectory generation requires substantial computation time.

This becomes increasingly demanding in networks with diverse train parameters and dynamic operating conditions. Scaling the approach to high-frequency corridors with rapid decision-making requirements remains a challenge.

Second, the selection of driving strategies for the initial Train Path Slot computation follows the most common and logical approaches in train trajectory optimisation, reflecting realistic ATO deployment strategies. These representative strategies define upper and lower bounds for multiple possible train trajectories with a fixed arrival time. Maximal Coasting (MC) (Scheepmaker et al., 2020) could serve as an alternative to EETC, further widening the Train Path Slot by extending its lower bound. Since MC applies maximum acceleration until reaching the speed limit, cruising at the speed limit, followed by a coasting regime, it may lead to earlier conflicts with the preceding train, potentially changing the location of the critical block and affecting the determination of intermediate TPs. The disadvantage is that the wider Train Path Slot could require additional TPs to ensure conflict-free operations. In addition, this study assumes fixed target arrival times. Future research could explore whether allowing arrival time windows may help resolve conflicts in certain cases, provided that it does not compromise punctuality and other operational requirements.

Finally, the current method focuses on TPE computation in a static environment based on a predefined timetable but can be extended to dynamic situations, where TPEs adapt to real-time traffic conditions and operational uncertainties. Future extensions may incorporate continuous updates, allowing TPEs to dynamically adjust based on real-time traffic plan changes from the TMS, status reports from the ATO onboard, and stochastic disturbances or disruptions. This would further contribute to a more adaptive and resilient ATO-driven, TMS-integrated railway digitalisation framework.

6. Conclusion

This paper introduced a novel method for optimising Timing Points (TPs) and generating Train Path Envelopes (TPEs), ensuring effective and conflict-free Automatic Train Operation (ATO) for a given real-time traffic plan. The optimised TPs within a TPE serve as constraints for onboard train trajectory generation, thereby aligning speed-based train operation with the timetable-based traffic management.

A key contribution of this work is the introduction of the Train Path Slot concept, which defines a bandwidth of track occupation times corresponding to multiple train driving strategies. Using this approach, we demonstrated that a (re)scheduled timetable may still contain train path conflicts, as conventional (re)scheduling algorithms typically assume a single deterministic train trajectory. Consequently, achieving conflict-free train operations requires intermediate TPs at strategic locations rather than solely relying on scheduled target departure and arrival times at stations.

To identify and avoid these conflicts, we formulated a two-step optimisation process, in which a Linear Programming model was developed to derive conflict-free Train Path Slots, which are subsequently applied as blocking time constraints to compute the TPEs. The proposed method was verified in various experiments and validated on one of the busiest Dutch railway corridors with a half-hourly periodic timetable. The real-life case study results demonstrated that introducing intermediate TPs at the beginning of blocks with the most significant overlapping blocking times effectively resolved conflicts and outperformed other alternatives. Moreover, the case study confirmed that the proposed TPE generation method was able to detect and eliminate all train path conflicts by adding a minimal number of TPs per train, and thus preventing unnecessary braking and reducing energy consumption by 29.75% for the affected train run.

Future research on TP optimisation will focus on the dynamic adjustment of TPEs based on real-time traffic plan or train status updates. Additionally, alternative train driving strategies, such as incorporating regenerative braking, may be explored as extensions of the proposed method. While these extensions enhance operational efficiency, they do not modify the underlying modelling framework established in this study.

CRediT authorship contribution statement

Ziyulong Wang: Writing – review & editing, Writing – original draft, Visualization, Validation, Software, Methodology, Investigation, Formal analysis, Data curation, Conceptualization. **Egidio Quaglietta:** Writing – review & editing, Supervision, Methodology, Conceptualization. **Maarten G.P. Bartholomeus:** Writing – review & editing, Supervision, Project administration, Conceptualization. **Alex Cunillera:** Writing – review & editing, Visualization, Software, Methodology. **Rob M.P. Goverde:** Writing – review & editing, Supervision, Project administration, Methodology, Funding acquisition, Conceptualization.

Declaration of competing interest

The authors declare that they have no known competing financial interests or personal relationships that could have appeared to influence the work reported in this paper.

Acknowledgements

This project has received funding from the Europe's Rail Joint Undertaking under the European Union's Horizon 2022 research and innovation programme under grant agreement No. 101101973 (FP1 - MOTIONAL). The authors also thank Dick Middelkoop and Vincent Weeda from ProRail for providing the data in this study.

References

Albrecht, A. R., Howlett, P. G., Pudney, P. J., Vu, X., & Zhou, P. (2015). Energy-efficient train control: The two-train separation problem on level track. *Journal of Rail Transport Planning & Management*, *5*(3), 163–182.

Albrecht, A. R., Howlett, P. G., Pudney, P. J., Vu, X., & Zhou, P. (2016a). The key principles of optimal train control—Part 1: Formulation of the model, strategies of optimal type, evolutionary lines, location of optimal switching points. *Transportation Research Part B: Methodological*, *94*, 482–508.

Albrecht, A. R., Howlett, P. G., Pudney, P. J., Vu, X., & Zhou, P. (2016b). The key principles of optimal train control—Part 2: Existence of an optimal strategy, the local energy minimization principle, uniqueness, computational techniques. *Transportation Research Part B: Methodological*, *94*, 509–538.

Albrecht, T., Binder, A., & Gassel, C. (2013). Applications of real-time speed control in rail-bound public transportation systems. *IET Intelligent Transport Systems*, *7*(3), 305–314.

Bešinović, N., Goverde, R. M. P., & Quaglietta, E. (2017). Microscopic models and network transformations for automated railway traffic planning. *Computer-Aided Civil and Infrastructure Engineering*, *32*(2), 89–106.

Caimi, G., Chudak, F., Fuchsberger, M., Laumanns, M., & Zenklusen, R. (2011). A new resource-constrained multicommodity flow model for conflict-free train routing and scheduling. *Transportation Science*, *45*(2), 212–227.

Corman, F., D'Ariano, A., Pacciarelli, D., & Pranzo, M. (2010). A tabu search algorithm for rerouting trains during rail operations. *Transportation Research Part B: Methodological*, *44*(1), 175–192.

Corman, F., & Meng, L. (2015). A review of online dynamic models and algorithms for Railway Traffic Management. *IEEE Transactions on Intelligent Transportation Systems*, *16*(3), 1274–1284.

Dong, H., Liu, X., Zhou, M., Zheng, W., Xun, J., Gao, S., Song, H., Li, Y., & Wang, F.-Y. (2022). Integration of train control and online rescheduling for High-Speed railways in case of emergencies. *IEEE Transactions on Computational Social Systems*, *9*(5), 1574–1582.

Dong, H., Ning, L., Zhou, M., Song, H., & Bai, W. (2024). Deep reinforcement learning for integration of train trajectory optimization and timetable rescheduling under disturbances. *IEEE Transactions on Neural Networks and Learning Systems*, *Early Access*, Available: https://doi.org/10.1109/TNNLS.2024.3357494.

EU-RAIL (2022). Europe's rail master plan. URL https://rail-research.europa.eu/wp-content/uploads/2022/03/EURAIL_Master-Plan.pdf.

EU-RAIL (2024). TMS and ATO/C-DAS timetable test & simulation environment. MOTIONAL Deliverable 15.2.

Goverde, R. M. P., Bešinović, N., Binder, A., Cacchiani, V., Quaglietta, E., Roberti, R., & Toth, P. (2016). A three-level framework for performance-based railway timetabling. *Transportation Research Part C: Emerging Technologies*, *67*, 62–83.

Goverde, R. M. P., Corman, F., & D'Ariano, A. (2013). Railway line capacity consumption of different railway signalling systems under scheduled and disturbed conditions. *Journal of Rail Transport Planning & Management*, *3*(3), 78–94.

Goverde, R. M. P., Scheepmaker, G. M., & Wang, P. (2021). Pseudospectral optimal train control. *European Journal of Operational Research*, *292*(1), 353–375.

Goverde, R. M. P., Su, S., & Tian, Z. (2023). Energy-efficient train operation: Conclusions and future work. In *Energy-efficient train operation: a system approach for railway networks* (pp. 229–234). Cham: Springer.

Haahr, J. H., Pisinger, D., & Sabbaghian, M. (2017). A dynamic programming approach for optimizing train speed profiles with speed restrictions and passage points. *Transportation Research Part B: Methodological*, *99*, 167–182.

Hou, Z., Dong, H., Gao, S., Nicholson, G., Chen, L., & Roberts, C. (2019). Energy-saving metro train timetable rescheduling model considering ATO profiles and dynamic passenger flow. *IEEE Transactions on Intelligent Transportation Systems*, *20*(7), 2774–2785.

Howlett, P. G., Pudney, P., & Albrecht, A. R. (2023). Optimal driving strategies for a fleet of trains on level track with prescribed intermediate signal times and safe separation. *Transportation Science*, *57*(2), 399–423.

Huang, Y., Yang, L., Tang, T., Gao, Z., Cao, F., & Li, K. (2018). Train speed profile optimization with on-board energy storage devices: A dynamic programming based approach. *Computers & Industrial Engineering*, *126*, 149–164.

Jansson, E., Olsson, N. O., & Fröidh, O. (2023). Challenges of replacing train drivers in driverless and unattended railway mainline systems—A Swedish case study on delay logs descriptions. *Transportation Research Interdisciplinary Perspectives*, *21*, Article 100875.

Li, S., Liu, R., Gao, Z., & Yang, L. (2021). Integrated train dwell time regulation and train speed profile generation for automatic train operations on high-density metro lines: A distributed optimal control method. *Transportation Research Part B: Methodological*, *148*, 82–105.

Li, Z., Yin, J., Chai, S., Tang, T., & Yang, L. (2023). Optimization of system resilience in urban rail systems: Train rescheduling considering congestions of stations. *Computers & Industrial Engineering*, *185*, Article 109657.

Liu, X., Dabiri, A., Xun, J., & De Schutter, B. (2023). Bi-level model predictive control for metro networks: Integration of timetables, passenger flows, and train speed profiles. *Transportation Research Part E: Logistics and Transportation Review*, *180*, Article 103339.

Long, S., Meng, L., Wang, Y., Miao, J., Luan, X., & Corman, F. (2023). Integrated speed modeling and traffic management to precisely model the effect and dynamics of temporary speed restrictions to high-speed railway traffic. *Transportation Research Part C: Emerging Technologies*, *152*, Article 104148.

Luan, X., Wang, Y., De Schutter, B., Meng, L., Lodewijks, G., & Corman, F. (2018a). Integration of real-time traffic management and train control for rail networks - Part 1: Optimization problems and solution approaches. *Transportation Research Part B: Methodological*, *115*, 41–71.

Luan, X., Wang, Y., De Schutter, B., Meng, L., Lodewijks, G., & Corman, F. (2018b). Integration of real-time traffic management and train control for rail networks - Part 2: Extensions towards energy-efficient train operations. *Transportation Research Part B: Methodological*, *115*, 72–94.

Mo, P., Yang, L., & Gao, Z. (2019). Energy-Efficient train operation strategy with speed profiles selection for an Urban Metro Line. *Transportation Research Record*, *2673*(4), 348–360.

Nash, C. A., Smith, A. S. J., Van de Velde, D., Mizutani, F., & Uranishi, S. (2014). Structural reforms in the railways: Incentive misalignment and cost implications. *Research in Transportation Economics*, *48*, 16–23.

Pachl, J. (2014). Timetable design principles. In I. A. Hansen, & J. Pachl (Eds.), *Railway timetabling & operations: analysis, modelling, optimisation, simulation, performance evaluation* (pp. 13–46). Hamburg: Eurail Press.

Pellegrini, P., Marlière, G., & Rodriguez, J. (2014). Optimal train routing and scheduling for managing traffic perturbations in complex junctions. *Transportation Research Part B: Methodological*, *59*, 58–80.

Quaglietta, E., Pellegrini, P., Goverde, R. M. P., Albrecht, T., Jaekel, B., Marlière, G., Rodriguez, J., Dollevoet, T., Ambrogio, B., Carcasole, D., Giaroli, M., & Nicholson, G. (2016). The ON-TIME real-time railway traffic management framework: A proof-of-concept using a scalable standardised data communication architecture. *Transportation Research Part C: Emerging Technologies*, *63*, 23–50.

Rao, X., Montigel, M., & Weidmann, U. (2016). A new rail optimisation model by integration of traffic management and train automation. *Transportation Research Part C: Emerging Technologies*, *71*, 382–405.

Scheepmaker, G. M., & Goverde, R. M. P. (2020). Energy-efficient train control using nonlinear bounded regenerative braking. *Transportation Research Part C: Emerging Technologies*, *121*, Article 102852.

Scheepmaker, G. M., Goverde, R. M. P., & Kroon, L. G. (2017). Review of energy-efficient train control and timetabling. *European Journal of Operational Research*, *257*(2), 355–376.

Scheepmaker, G. M., Willeboordse, H. Y., Hoogenraad, J. H., Luijt, R. S., & Goverde, R. M. P. (2020). Comparing train driving strategies on multiple key performance indicators. *Journal of Rail Transport Planning & Management*, *13*, Article 100163.

UIC (2013). *Code 406 – capacity* (2nd ed.). Paris: International Union of Railway.

UNISIG (2023). ERTMS/ATO - System requirements specification. SUBSET-125.

Wang, P., & Goverde, R. M. P. (2016). Multiple-phase train trajectory optimization with signalling and operational constraints. *Transportation Research Part C: Emerging Technologies*, *69*, 255–275.

Wang, P., & Goverde, R. M. P. (2017). Multi-train trajectory optimization for energy efficiency and delay recovery on single-track railway lines. *Transportation Research Part B: Methodological*, *105*, 340–361.

Wang, P., & Goverde, R. M. P. (2019). Multi-train trajectory optimization for energy-efficient timetabling. *European Journal of Operational Research*, *272*(2), 621–635.

Wang, P., Trivella, A., Goverde, R. M. P., & Corman, F. (2020). Train trajectory optimization for improved on-time arrival under parametric uncertainty. *Transportation Research Part C: Emerging Technologies*, *119*, Article 102680.

Wang, P., Zhu, Y., & Corman, F. (2022). Passenger-centric periodic timetable adjustment problem for the utilization of regenerative energy. *Computers & Industrial Engineering*, *172*, Article 108578.

Wang, Y., Zhu, S., Li, S., Yang, L., & De Schutter, B. (2022). Hierarchical model predictive control for on-line high-speed railway delay management and train control in a dynamic operations environment. *IEEE Transactions on Control Systems Technology*, *30*(6), 2344–2359.

Wang, Z., Quaglietta, E., Bartholomeus, M. G. P., & Goverde, R. M. P. (2022). Assessment of architectures for automatic train operation driving functions. *Journal of Rail Transport Planning & Management*, *24*, Article 100352.

Yin, J., Tang, T., Yang, L., Xun, J., Huang, Y., & Gao, Z. (2017). Research and development of automatic train operation for railway transportation systems: A survey. *Transportation Research Part C: Emerging Technologies*, *85*, 548–572.

Ying, P., Zeng, X., D'Ariano, A., Pacciarelli, D., Song, H., & Shen, T. (2023). Quadratically Constrained Linear Programming-based energy-efficient driving for High-speed Trains with neutral zone and time window. *Transportation Research Part C: Emerging Technologies*, *154*, Article 104202.

Zhan, S., Xie, J., Wong, S., Zhu, Y., & Corman, F. (2024). Handling uncertainty in train timetable rescheduling: A review of the literature and future research directions. *Transportation Research Part E: Logistics and Transportation Review*, *183*, Article 103429.

Zhang, Y., D'Ariano, A., He, B., & Peng, Q. (2019). Microscopic optimization model and algorithm for integrating train timetabling and track maintenance task scheduling. *Transportation Research Part B: Methodological*, *127*, 237–278.